Robotica (2008) volume 26, pp. 19–39. © 2007 Cambridge University Press
doi:10.1017/S0263574707003554 Printed in the United Kingdom

Kinematic and dynamic performance analysis of artificial legged systems

Manuel F. Silva* and J. A. Tenreiro Machado

Department of Electrical Engineering, Institute of Engineering of Porto, Rua Dr. António Bernardino de Almeida, 4200-072 Porto, Portugal.

(Received in Final Form: May 8, 2007. First published online: June 22, 2007)

SUMMARY

This paper studies the mechanical configuration and the periodic gaits of multi-legged locomotion systems based on its kinematic and dynamic models. The purpose is to determine the system performance during walking, and the best set of locomotion variables that minimize a set of optimization indices. In this perspective, two kinematic and four dynamic indices are formulated to quantitatively measure the performance of the walking robot. The kinematic indices consist of the perturbation analysis and the locomobility measure, and the dynamic performance indices of the walking robot locomotion are the mean absolute density of energy, the mean power density dispersion, the density of power lost and the mean force at the body-legs interface. A set of model-based simulation experiments reveals the system configuration and the type of movements that lead to a better performance, for a specific locomotion mode, from the viewpoint of the proposed indices.

KEYWORDS: Robotics; Walking; Legged locomotion; Dynamic modelling; Kinematics; Simulation.

1. Introduction

Legged robots present significant advantages because they allow locomotion in terrain inaccessible to traditional vehicles, since they do not need a continuous support surface. However, in the present state of development of artificial locomotion systems, there are several aspects that have to be necessarily improved and optimized (Silva and Machado, 2007). Different optimization strategies have been proposed and applied to these systems, either during its design and construction phase, or during its operation. Researchers paid attention to the gait selection, and to its adaptation to the terrain and locomotion conditions (Yang, 2006). Among the several criteria followed by distinct authors, one may include aspects related to energy efficiency, stability (Zhou, 2003; Garcia and de Santos, 2005), velocity, comfort, mobility and environmental impact.

With these facts in mind, a simulation model was developed for multi-leg locomotion systems, including several periodic gaits (Silva *et al.*, 2005). This study intends to generalize previous work (Silva *et al.*, 2002a; Silva *et al.*, 2002b; Silva *et al.*, 2003) and, in this perspective, several kinematic and dynamic measures of the robotic locomotion system performance are formulated. At the kinematic level, indices of the feet trajectories perturbation are established that measure the sensitivity of the feet cartesian trajectories to disturbances in the joints variables, and the indices of body and feet trajectories locomobility that give an indication of the mechanical capability to implement the desired robot motion. At the dynamic level, four performance measures are implemented, namely the mean absolute density of energy during locomotion, the mean power density dispersion, the density of lost power in the joint actuators and the mean force at the body–legs interface, all these indices being evaluated along the locomotion cycle.

The foot and body trajectories are analyzed with respect to its variation with the gait, duty factor, step length, maximum foot clearance, body height, leg links length and foot trajectory offset. Several simulation experiments reveal the system configuration and the type of movements that lead to a better mechanical implementation, for a given locomotion mode, from the viewpoint of the proposed indices.

Bearing these facts in mind, the remainder of this paper is organized as follows. Section 2 presents some of the strategies and criteria that have been used to increase the efficiency of legged robots. Section 3 introduces the model for a multi-legged robot and the motion planning algorithms. Section 4 formulates the optimizing kinematic and dynamic indices, while Section 5 develops a set of experiments that reveal the influence of the system parameters in the periodic gaits. Section 6 discusses the main results of this study. Finally, Section 7 presents the main conclusions and some work lines that are open in this research area.

2. State-of-the-Art Multi-Legged Robot Optimization

Several strategies and criteria have been used with the final goal of increasing the efficiency of artificial locomotion systems.

Since legged locomotion robots are inspired in animals observed in nature, a frequent approach to their design and construction is to make a mechatronic mimic of the animal that is intended to replicate, either in terms of its physical dimensions, or in terms of characteristics such as the gait and the actuation of the limbs (Laksanacharoen *et al.*, 2000; Witte *et al.*, 2001a; Witte *et al.*, 2001b).

Evolutionary strategies are an alternative way of imitating nature. Animals characteristics are not directly copied, but instead, it copies the process that nature conceives for its generation and evolution.

* Corresponding author. E-mail: mss@isep.ipp.pt

https://doi.org/10.1017/S0263574707003554 Published online by Cambridge University Press

One possibility to implement this idea makes use of genetic algorithms as an engine to generate robot structures (Farritor *et al*., 1996; Leger, 2000). In the literature, there are also descriptions of research in which evolutionary strategies are adopted to optimize the structure of a specific robot (Juárez-Guerrero *et al*., 1998; Ishiguro *et al*., 2002).

The previous approaches to artificial locomotion systems design are based on the strategies found in nature. However, it is important to keep in mind that legged robots are machines and, therefore, the first aspect to consider in their design phase should be the correct implementation from the mechanical and physical viewpoint.

Following this line of thought, Habumuremyi and Doroftei (2001) present the characteristics of several structures that can be adopted for the legs of artificial locomotion systems. Hirose and Arikawa (2000) present a set of concepts to be adopted during the design of legged vehicles in order to maximize the power developed in the system and maximize the energy efficiency. In certain situations, approaches to the robot design based on empirical knowledge of the areas of mechanics and physics are also adopted. In these cases, the equipments are designed with the objective of minimizing some situations that penalize the performance of the robot under consideration (Hirose *et al*., 1997; Yamaguchi and Takanishi, 1998).

Concerning the weakness of artificial locomotion systems, one of the most serious problems facing the designers is the optimization of the energy consumption. It is verified that the locomotion efficiency of the existing robots is low, either when compared with the living animals, or with the locomotion through wheels. For example, Kajita *et al*. (2002) performed a simulation study of the HRP1 humanoid robot running gait and concluded that the robot would need actuators 28 up to 56 times more powerful than those available in the real humanoid. Besides this, they also estimated that the energy consumption would be about ten times higher than the energy required by a human adopting the same gait.

Researchers expect that, in future, locomotion through artificial legs would become one of the most efficient transportation modes from the energy viewpoint. This implies that great attention should be devoted to this aspect in the development of these sort of systems, namely, through the use of energy-based optimization criteria, since this influences the choice of the mechanical structure, propulsion method and power supply. Moreover, there is an important hypothesis that seems to explain most of the legs and body motions during human locomotion. This hypothesis states that during locomotion humans control their muscles activity, moving the various body segments in such a way that the metabolic energy needed to travel a certain distance is minimized (Neuhaus and Kazerooni, 2000). It is also recognized that locomotion in most of the legged animals optimize the energy efficiency in detriment to the motion smoothness (Alexander, 1984).

Based on these ideas, several authors developed optimization studies of artificial locomotion structures and of their gaits, based on energy criteria.

An index used frequently to analyze and compare the performance of legged robots is the specific resistance (ρ). This index, originally introduced by Gabrielli and Von Kármán (1950), to compare the locomotion efficiency of different sorts of vehicles, is based on the vehicle maximum power and on the maximum velocity that it can reach. The specific resistance was alternatively defined by Lasa and Buehler (2001) as a function of the traveling velocity.

This index is adopted to study the performance of a passive biped robot when compliance is introduced into its joints (Linde, 1998). It is also used to compare the performance of the RHex hexapod when crossing obstacles (Saranli *et al*., 2001) or when going up and down the stairs (Moore *et al*., 2002; Campbell and Buehler, 2003). Lasa and Buehler (2001) also adopt this metric to analyze the performance of the SCOUT-II quadruped with reduced actuation.

Some authors pointed out that, in opposition to the use of the mechanical power for computing the specific resistance, the index should be computed using the electric power, in order to be able to consider several significant energy losses that occur in the systems (Saranli *et al*., 2001; Lasa and Buehler, 2001; Campbell and Buehler, 2003). This gives rise to an alternative definition for the specific resistance (Linde, 1998; Moore *et al*., 2002). To prove their statement, Lasa and Buehler (2001) computed the mechanical and electrical power of the SCOUT-II robot, the electric power being approximately ten times higher than the mechanical power. This result is also reflected in the specific resistance that these authors compute using the electric and the mechanical power.

A different approach is performed by Lapshin (1995) that estimates the energy consumption of legged vehicles moving along straight trajectories, using statically stable locomotion gaits. Marhefka and Orin (1997) simulate a hexapod robot to study how the locomotion parameters affect the energy consumption. Zhoga (1998) analyzes the energy consumption of an eight-legged system, deducing the equations for its energy consumption from the dynamic model, and compares it with the energy consumptions of machines with equivalent dimensions, but using wheels and tracks. Finally, Briskin *et al*. (2003) adopted the energy consumption computed from the dynamic model for the optimization and performance analysis of the walking chassis for multipurposes robot.

Pedroche *et al*. (2003) went even further and presented a detailed model of the energy consumption of legged robots based on the robot dynamics and the actuators model (including the electrical and mechanical parts). This model is later applied in order to analyze the energy consumption of the SILO4 quadruped under distinct conditions.

Besides the several criteria to optimize the legged robots previously mentioned, other approaches have also been sporadically used. One of them is based in the manipulability ellipsoids (Yoshikawa, 1990). Indices based in this concept have been adopted by Koyachi *et al*. (1997) in the optimization of the MELMANTIS-1 and MELMANTIS-2 hexapods, by Takeuchi (1999) in the design of the front and rear legs of the MEL HORSE II and by Kang *et al*. (2003) during the design of the MRWALLSPECT-III climbing robot to determine the optimum legs link lengths.

3. A Model for Multilegged Locomotion

In our work, we consider a longitudinal walking system with n legs ($n \geq 2$ and n even), with the legs equally distributed

https://doi.org/10.1017/S0263574707003554 Published online by Cambridge University Press

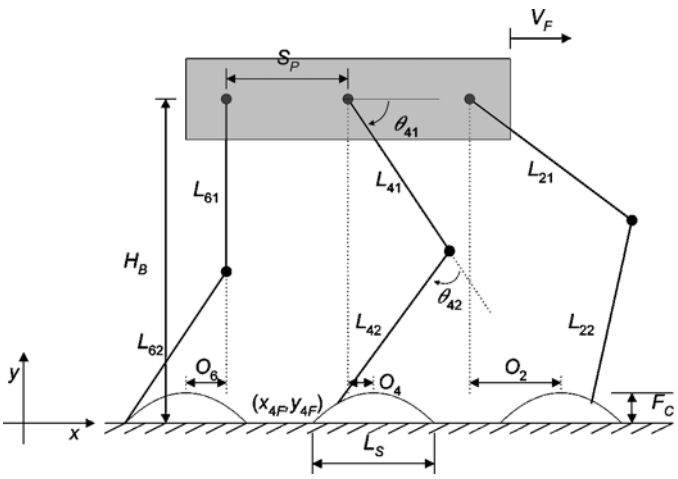


Fig. 1. Coordinate system and variables that characterize the motion trajectories of the multi-legged robot.

along both sides of the robot body, each having two rotational joints (i.e., $j = \{1, 2\} \equiv \{\text{hip, knee}\}$) (Fig. 1) (Silva *et al.*, 2005). The even legs are on the left side of the robot body and the odd legs on the right side. All legs are numbered from the front of the robot to the back.

Motion is described by means of a world coordinate system. The kinematic model comprises: the cycle time T, the duty factor β, the transference time $t_T = (1 - \beta)T$, the support time $t_S = \beta T$, the step length L_S, the stroke pitch S_P, the body height H_B, the maximum foot clearance F_C, the ith leg lengths L_{i1} and L_{i2}, and the foot trajectory offset O_i ($i = 1, \ldots, n$). Moreover, we consider a periodic trajectory for each foot with body velocity $V_F = L_S/T$.

Gaits describe discontinuous sequences of leg movements, alternating between transfer and support phases and, in the simulation model, we consider the wave gait (WG), equal phase half cycle gait (EPHCG), equal phase full cycle gait (EPFCG), backward wave gait (BWG), backward equal phase half cycle gait (BEPHCG), and backward equal phase full cycle gait (BEPFCG) (Silva *et al.*, 2005). Given a particular gait and duty factor β, it is possible to calculate, for leg i, the corresponding phase ϕ_i, the time instant where each leg leaves and returns to contact with the ground, and the cartesian trajectories of the tip of the feet (that must be completed during t_T). Based on this data, the trajectory generator is responsible for producing a motion that synchronises and coordinates the legs.

The robot body, and by consequence each leg hip, is assumed to have a desired horizontal movement with a constant forward speed V_F. Therefore, for leg i the cartesian coordinates of the hip of the legs are given by $\mathbf{p_{Hd}}(t) = [x_{iHd}(t),\ y_{iHd}(t)]^{\mathrm{T}}$

$$\mathbf{p_{Hd}}(t) = [V_F t + Sp(1 - \text{ceil}(i/2))\ H_B]^{\mathrm{T}}, \qquad i = 1, 2, \ldots, n \quad (1)$$

where ceil(x) rounds x to the nearest integer towards infinity.

For each walking cycle, the desired trajectory of the swing leg foot is computed through a cycloid function (Eq. 2). For example, considering that the transfer phase starts at $t = 0$ s for leg $i = 1$ we have for $\mathbf{p_{Fd}}(t) = [x_{iFd}(t),\ y_{iFd}(t)]^{\mathrm{T}}$

- during the transfer phase:

$$\mathbf{p_{Fd}}(t) = \left[V_F\left[t - \frac{t_T}{2\pi}\sin\left(\frac{2\pi t}{t_T}\right)\right],\ \frac{F_C}{2}\left[1 - \cos\left(\frac{2\pi t}{t_T}\right)\right]\right]^T. \quad (2a)$$

- during the stance phase:

$$\mathbf{p_{Fd}}(t) = [V_F T \quad 0]^{\mathrm{T}}. \quad (2b)$$

The algorithm for the motion planning accepts the desired cartesian trajectories of the leg hips $\mathbf{p_{Hd}}(t)$ and feet $\mathbf{p_{Fd}}(t)$ as inputs and, through an inverse kinematics algorithm ψ^{-1}, generates the related joint trajectories $\mathbf{\Theta_d}(t) = [\theta_{i1d}(t), \theta_{i2d}(t)]^{\mathrm{T}}$

$$\mathbf{p_d}(t) = [x_{id}(t) \quad y_{id}(t)]^{\mathrm{T}} = \mathbf{p_{Fd}}(t) - \mathbf{p_{Hd}}(t) \quad (3a)$$

$$\mathbf{p_d}(t) = \boldsymbol{\psi}[\mathbf{\Theta_d}(t)] \Rightarrow \mathbf{\Theta_d}(t) = \boldsymbol{\psi}^{-1}[\mathbf{p_d}(t)] \quad (3b)$$

$$\dot{\mathbf{\Theta}}_\mathbf{d}(t) = \mathbf{J}^{-1}[\dot{\mathbf{p}}_\mathbf{d}(t)],\ \mathbf{J} = \frac{\partial \boldsymbol{\psi}}{\partial \mathbf{\Theta_d}}. \quad (3c)$$

In order to avoid the impact and friction effects, at the planning phase we estimate null velocities of the feet in the instants of landing and taking off, also assuring the velocity continuity. These joint trajectories can also be accomplished either with an acceleration having a stepwise or a polynomial *versus* time profile.

4. Measures for Locomotion Performance Evaluation

To evaluate the system operation and to allow the comparison among different strategies, there is a need to adopt performance measures. Therefore, in this section, several global measures of the system performance are formulated. The aim is to verify whether a correlation between different viewpoints can be found during robot locomotion. These performance measures are grouped into two, according to whether they make use of the robot kinematic or the dynamic models.

4.1. Kinematic indices

4.1.1. Perturbation analysis. The essence of locomotion is to move smoothly a section of the body from one place to another with some restrictions in terms of execution time.

In many practical cases, the robotic system is "noisy", i.e. has internal or external disturbing forces. As such, an approach entitled "perturbation analysis" is implemented to determine how the robot model stands with trajectory variations. First, the joint trajectories are computed by the inverse kinematics algorithm. Later, the joint accelerations are "corrupted" by a small amplitude uniform distribution noise with zero mean that is added to the signal. The resulting joint leg trajectories (and the feet cartesian trajectories) suffer some distortion and differ from the desired ones. By

https://doi.org/10.1017/S0263574707003554 Published online by Cambridge University Press

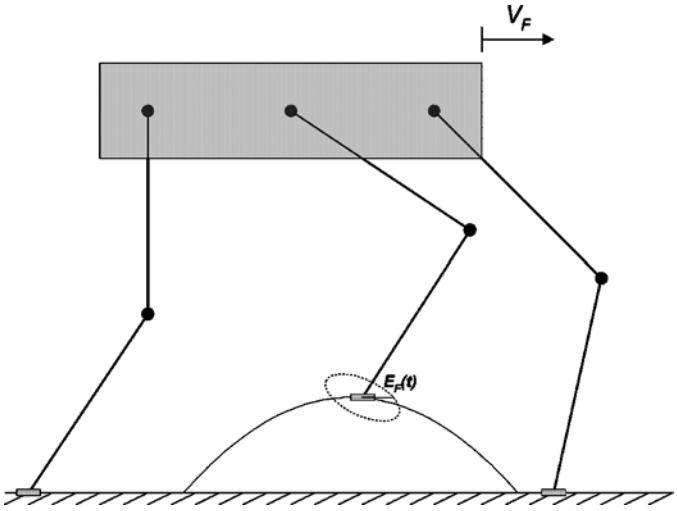


Fig. 2. Graphical representation of the distance among the centre of the ellipsoids and its intersections with the tangent to the trajectory of the foot (E_F).

computing the forward kinematics, we determine two indices based on the statistical average of the mean square error as

$$\xi_{\dot{x}} = \frac{1}{N_S}\sum_{i=1}^{N_S}\sqrt{\frac{1}{T}\frac{1}{n}\sum_{i=1}^{n}\int_0^T [\dot{x}_{iFn}(t) - \dot{x}_{iFd}(t)]^2\,\mathrm{d}t} \quad [\mathrm{ms}^{-1}] \tag{4a}$$

$$\xi_{\dot{y}} = \frac{1}{N_S}\sum_{i=1}^{N_S}\sqrt{\frac{1}{T}\frac{1}{n}\sum_{i=1}^{n}\int_0^T [\dot{y}_{iFn}(t) - \dot{y}_{iFd}(t)]^2\,\mathrm{d}t} \quad [\mathrm{ms}^{-1}] \tag{4b}$$

where N_S is the total number of steps for averaging purposes, $(\dot{x}_{iFd}, \dot{x}_{iFn})$ and $(\dot{y}_{iFd}, \dot{y}_{iFn})$ are the ith samples of the horizontal and vertical velocities, desired and "corrupted" with noise, on the robot foot, respectively. The stochastic perturbation penalises the system's performance, and we shall be concerned with minimising $\xi_{\dot{x}}$ and $\xi_{\dot{y}}$.

4.1.2. Locomobility measure. The motivation for the development of the locomobility index is to apply the concepts of arm manipulability (Yoshikawa, 1990) to multilegged walking. This performance measure can be expressed through the Jacobian matrix.

In the present case, the global indices are obtained by averaging the distance among the centre of the (small) ellipsoids and its intersections with the tangent to the desired trajectories (Fig. 2), either of the foot (E_F) or of the robot body (E_B), over a complete locomotion cycle T, originating at the foot (L_F) and body (L_B) locomobility indices, respectively, as

$$L_F = \frac{1}{T}\int_0^T E_F(t)\,\mathrm{d}t \quad [\mathrm{m}] \tag{5a}$$

$$L_B = \frac{1}{T}\int_0^T E_B(t)\,\mathrm{d}t \quad [\mathrm{m}]. \tag{5b}$$

In this perspective, the most suitable trajectory is the one that maximises L_F and L_B.

4.2. Dynamic indices

4.2.1. Mean absolute density of energy. The key measure in this analysis is the mean absolute density of energy per travelled distance E_{av}. This index is computed assuming that energy regeneration is not available by actuators doing negative work, i.e. by taking the absolute value of the mechanical power. This reasoning in based on the verification that on biological beings, the energy that is involved in the limbs motion through muscular actuation does not have the possibility of being recovered during the time intervals in which the work is negative. As such, at the biological level, the trajectory planning only promotes one direction in the nutrients supply.

At a given leg i ($i = 1, \ldots, n$) and joint j ($j = 1, \ldots, m$), the mechanical power is the product of the actuator torque and angular velocity. As a consequence, the index E_{av} is obtained by averaging the mechanical absolute energy delivered over the travelled distance d as

$$E_{av} = \frac{1}{d}\sum_{i=1}^{n}\sum_{j=1}^{m}\int_0^T |\boldsymbol{\tau}_{ij}(t)\dot{\boldsymbol{\theta}}_{ij}(t)|\,\mathrm{d}t \quad [\mathrm{Jm}^{-1}] \tag{6}$$

where τ_{ij} is the motor torque and $\dot{\theta}_{ij}$ represents the joint velocity. Therefore, a good performance of the system requires the minimisation of E_{av}.

4.2.2. Mean power density dispersion. The power minimisation is an important consideration, but instants with very high power demands may occur. In such cases, the average value can be small while the peaks are physically unrealisable. Therefore, an alternative index is the standard deviation per meter that evaluates the power variability (or dispersion) over a complete cycle T and travelled distance d

$$D_{av} = \frac{1}{d}\sqrt{\frac{1}{T}\int_0^T [P_t(t) - P_0]^2\,\mathrm{d}t} \quad [\mathrm{Wm}^{-1}] \tag{7a}$$

$$P_t(t) = \sum_{i=1}^{n} P_i(t) \quad [\mathrm{W}] \tag{7b}$$

$$P_i(t) = \sum_{j=1}^{m} |\boldsymbol{\tau}_{ij}(t)\dot{\boldsymbol{\theta}}_{ij}(t)| \quad [\mathrm{W}] \tag{7c}$$

$$P_0 = \frac{E_{av}}{T}\,\mathrm{d}_1, \quad \text{with} \quad \mathrm{d}_1 = 1\,\mathrm{m} \quad [\mathrm{W}] \tag{7d}$$

where P_i is the instantaneous absolute mechanical power on leg i, and P_t the total instantaneous absolute mechanical power. The constant P_0 represents the mean absolute density of power enrolled in the travel of 1 m and $P_t(t) - P_0$ represents the instantaneous deviation relative to that value. Another value may be considered for P_0, i.e. another constant in relation to which the deviations are measured. For example, another choice for P_0 can be the average value of the total instantaneous mechanical power along the locomotion cycle, considering that the energy flow in the actuators are

https://doi.org/10.1017/S0263574707003554 Published online by Cambridge University Press

bidirectional. However, for a consistency reason, in this work we decided to use a term based on E_{av} to compute this index.[1]

From this viewpoint, the most suitable trajectory is also the one that minimises D_{av}.

4.2.3. Density of power lost.[2] Another alternative optimisation strategy for an actuated system consists of T_L, the density of power lost in the joint actuators per travelled distance d. From this point of view, the index density of power lost per meter can be defined as

$$T_L = \frac{1}{d}\sqrt{\frac{1}{T}\sum_{i=1}^{n}\sum_{j=1}^{m}\int_0^T [\tau_{ij}(t)]^2\,\mathrm{d}t} \quad [\mathrm{N}]. \tag{8}$$

Once again, the most suitable trajectory is the one that minimises the index T_L.

4.2.4. Mean force at the body–legs interface.[3] A fourth possible optimisation strategy addresses the forces that occur on the hips of the robot per travelled distance d and time spent on travel T. The index mean force on hips per meter is defined as

$$F_L = \frac{1}{d}\sqrt{\frac{1}{T}\sum_{i=1}^{n}\int_0^T \{[f_{ix}(t)]^2 + [f_{iy}(t)]^2\}\,\mathrm{d}t} \quad [\mathrm{Nm}^{-1}]. \tag{9}$$

The best trajectory is the one that minimises F_L.

5. Analysis and Optimization of the Artificial Locomotion System Parameters

In this section, the results of a set of simulations are presented based on the robot model and the proposed indices. These simulations intend to analyse the influence of several parameters during multi-legged walking, when adopting several periodic gaits. The aim is to verify if it is possible to find a correlation among the different viewpoints during the robot locomotion.

In the experiments, the role of the gait *versus* the parameters β, L_S, H_B and F_C are examined considering the model and locomotion parameters presented in Table 1.

This study starts by considering the situation on which the robot presents the leg with a forward knee, as is common in mammals, while adopting the WG gait. After it is examined, the alternative leg structure with a backwards knee, common in birds, and the adoption of different periodic locomotion gaits is presented.

Table 1. System parameters.

Robot model parameters		Locomotion parameters	
n	6	β	50%
S_P	1.0 m	L_S	1.0 m
L_{ij}	0.5 m	H_B	0.9 m
O_i	0.0 m	F_C	0.1 m
M_b	88.0 kg	V_F	1.0 ms^{-1}
M_{ij}	1.0 kg		

Due to the high number of parameters and values, the following subsections present the optimal values by cross-relating several distinct combinations for the locomotion with the WG.

5.1. Kinematic analysis

We start the study of the kinematic indices by analysing the variation of the parameters duty factor (β) *versus* body height (H_B) for different values of the step length (L_S) and of the maximum foot clearance (F_C).

For the WG, the perturbation analysis (Fig. 3) reveals that the indices $\xi_{\dot{x}}$ and $\xi_{\dot{y}}$ increase with β particularly for $\beta >$ 90%. In what concerns the effect of H_B, the results for the two indices are contradictory. It is visible, in particular, for small values of β that $\xi_{\dot{x}}$ increases with H_B in opposition with $\xi_{\dot{y}}$ that decreases. These results remain the same for low values of L_S and F_C. For high values of L_S and F_C, the index $\xi_{\dot{x}}$ starts decreasing with H_B, keeping the variation of $\xi_{\dot{y}}$ its pattern. However, it should be mentioned that as the values of L_S and F_C increase, the allowable range of variation of the parameters β and H_B decreases.

Figure 4 shows that both $\xi_{\dot{x}}$ and $\xi_{\dot{y}}$ increase considerably with L_S but have a slight variation with F_C. The pattern depicted in Fig. 4 remains for different values of β and H_B.

Figures 3 and 4 point out that the locomotion should be performed with reduced values of the parameters β, L_S and F_C, but are not conclusive in what concerns the appropriate value of H_B.

In the sequel, this analysis is repeated using the foot and body locomotion indices.

From Figs. 5 and 6, we conclude that L_F and L_B present different variations with β and H_B. Regarding L_F we verify that it decreases sharply with β but varies slightly with H_B, presenting higher values for values of the body height near the maximum, independently of the values of L_S and F_C. The index L_B presents a more complex pattern. For reduced values of the step length, L_B increases sharply with H_B and slightly with β, as can be seen in Fig. 5. For higher values of L_S, the behaviour of this index is more complex. As the value of the parameter L_S increases, L_B starts decreasing with H_B for high values of β. In a similar way, as L_S increases, the index L_B decreases with β for high values of H_B. This variation becomes stronger when increasing L_S, as can be observed in Fig. 6, and is independent of the value of F_C.

[1] This subject is similar to the one found in statistics, with the variance $V = \frac{1}{N}\sum_i (x_i - \mu)^2$. Taking the average, μ only corresponds to minimize V since $\forall c \in \mathrm{R}$ we have $\frac{1}{N}\sum_i (x_i - c)^2 = \frac{1}{N}\sum_i (x_i - \mu)^2 + (c - \mu)^2$. In case of eq. (10a), it was also verified that other values for the constant P_0 did not change qualitatively the shape of the chart (Silva *et al.*, 2002a; Silva *et al.*, 2002b; Silva *et al.*, 2003).

[2] This index, entitled Density of Power Lost, is based on a definition associated to the power lost in electrical actuators; however, its dimensions are not those of power but, in fact, of a force having unit N.

[3] As in the previous case, this index has the name mean force at the body–legs interface, since its computation is based on the forces that appear at the robot hips, but its dimensions are those of a force by meter having unit Nm^{-1}.

https://doi.org/10.1017/S0263574707003554 Published online by Cambridge University Press

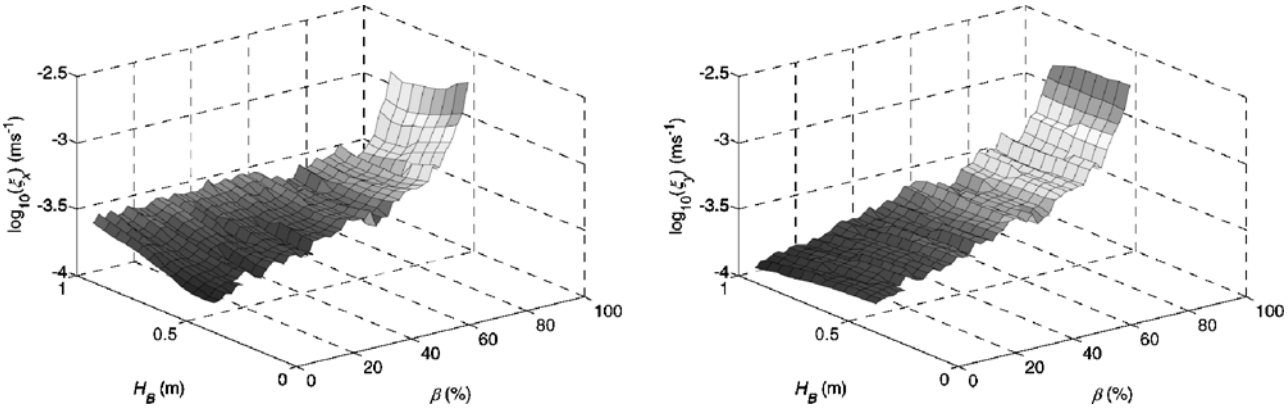


Fig. 3. Charts of $\log(\xi_{\dot{x}})$ and $\log(\xi_{\dot{y}})$ *vs.* (β, H_B) with $L_S = 1$ m, $F_C = 0.2$ m, WG.

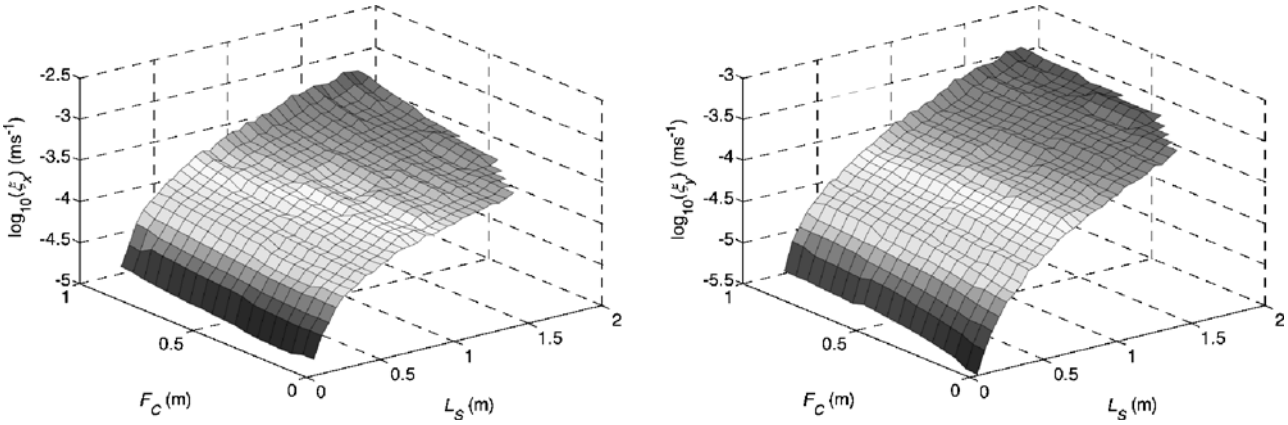


Fig. 4. Charts of $\log(\xi_{\dot{x}})$ and $\log(\xi_{\dot{y}})$ *vs.* (L_S, F_C) with $\beta = 50\%$, $H_B = 0.9$ m, WG.

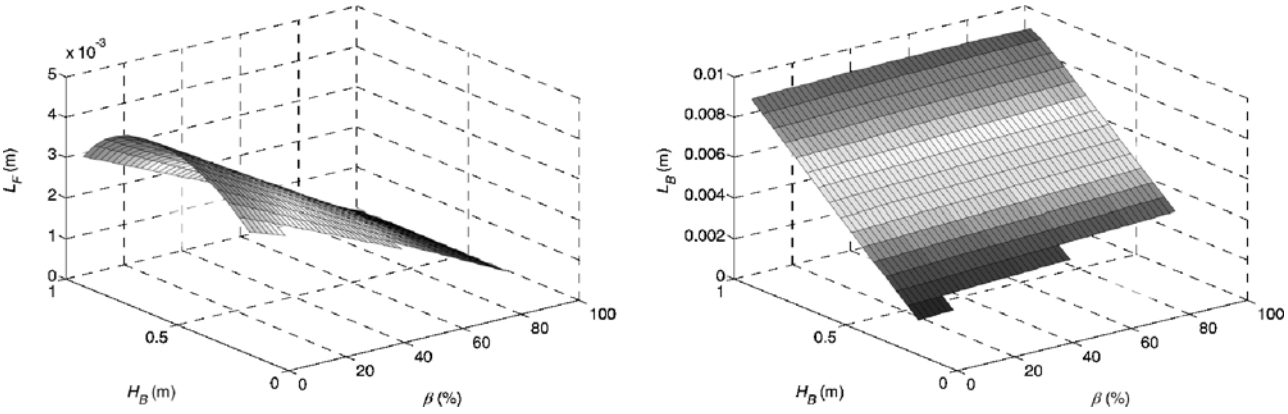


Fig. 5. Charts of L_F and L_B *vs.* (β, H_B) with $L_S = 0.2$ m, $F_C = 0.1$ m, WG.

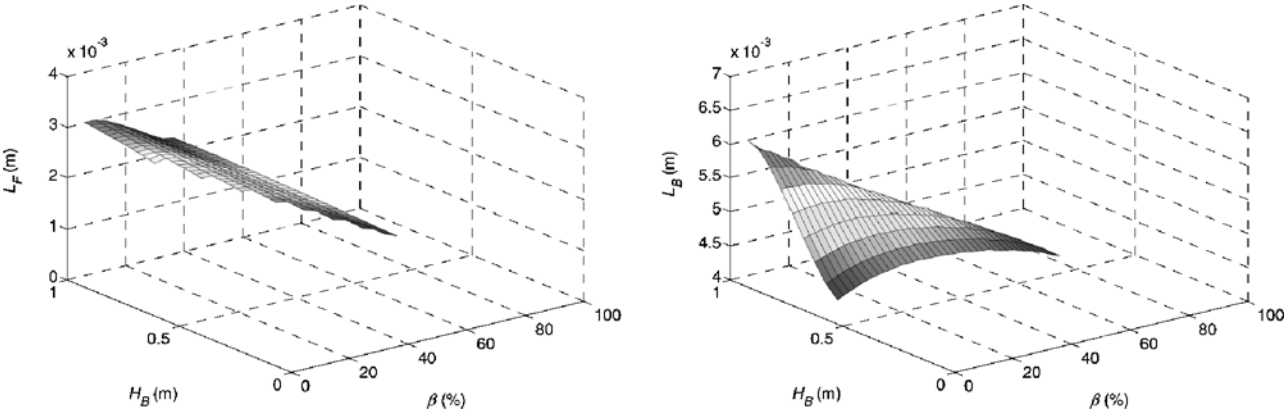


Fig. 6. Charts of L_F and L_B *vs.* (β, H_B) with $L_S = 2.0$ m, $F_C = 0.5$ m, WG.

https://doi.org/10.1017/S0263574707003554 Published online by Cambridge University Press

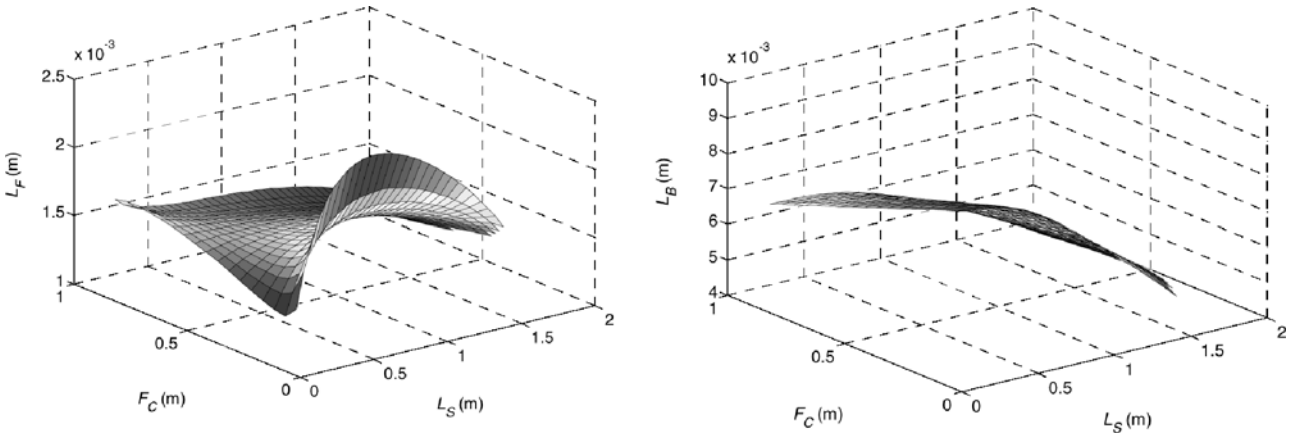


Fig. 7. Charts of L_F and L_B *vs.* (L_S, F_C) with $\beta = 50\%$, $H_B = 0.9$ m, WG.

Figure 7 shows the variation of the locomobility indices with L_S and F_C. For $F_C > 0.5$ m, L_F remains almost invariant with F_C but decreases sharply with L_S. For low values of F_C, this index presents a maximum for $L_S \approx 1.0$ m. The index L_B decreases sharply with L_S and slightly with F_C. The variation presented in Fig. 7 remains for different values of β and H_B.

From Figs. 5–7, it is possible to conclude that the robot should walk with the body in a relatively high position, except when the locomotion adopts a high value for β. Besides, the steps should be short and the foot should remain near the ground. These results are in agreement with those previously obtained through the perturbations analysis.

5.2. *Dynamic analysis*

The performance analysis is now extended by adopting the dynamic indices. Therefore, after planning the joint trajectories we calculate the inverse dynamics in order to "map" the kinematics into power consumption.

The simplified robot inverse dynamic model is of the form

$$\mathbf{\Gamma} = \mathbf{H}(\mathbf{\Theta})\ddot{\mathbf{\Theta}} + \mathbf{c}(\mathbf{\Theta}, \dot{\mathbf{\Theta}}) + \mathbf{g}(\mathbf{\Theta}) \tag{10}$$

where $\mathbf{\Gamma} = [f_{ix}, f_{iy}, \tau_{i1}, \tau_{i2}]^{\mathrm{T}}$ is the vector of forces/torques, $\mathbf{\Theta} = [x_{iH}, y_{iH}, \theta_{i1}, \theta_{i2}]^{\mathrm{T}}$ is the vector of position coordinates, $\mathbf{H}(\mathbf{\Theta})$ is the inertia matrix and $\mathbf{c}(\mathbf{\Theta}, \dot{\mathbf{\Theta}})$ and $\mathbf{g}(\mathbf{\Theta})$ are the vectors of centrifugal/Coriolis and gravitational forces/torques, respectively.

Figure 8 presents the charts of $\log(E_{av})$, $\log(D_{av})$, $\log(T_L)$ and $\log(F_L)$ *vs.* (β, H_B). We conclude that $\log(E_{av})$, $\log(D_{av})$ and $\log(T_L)$ present a similar shape, increasing monotonically with β and decreasing/increasing slightly with H_B for small/high values of β. The chart of $\log(D_{av})$ has the particularity of revealing the occurrence of a minimum for $\beta = 16\%$ and $H_B = 0.9$ m. The index F_L presents a slightly different variation. In fact, F_L is almost invariant with H_B, except for high values of β where it decreases slightly, while its variation with the duty factor presents a minimum for $\beta \approx 88\%$.

For low values of the step length and of the foot clearance, the charts of $\log(E_{av})$, $\log(D_{av})$, $\log(T_L)$ and $\log(F_L)$ *vs.* (β, H_B) do not present significant changes on its shape. The charts of $\log(E_{av})$, $\log(D_{av})$ and $\log(T_L)$ reveal a similar shape, increasing monotonically with β and varying slightly with H_B, showing each of them a minimum for $H_B \approx 0.65$ m. The chart of F_L presents a slightly different shape from the others, being practically invariant with H_B and revealing a minimum for $\beta \approx 80\%$.

In case we adopt higher values for the step length L_S, and for the maximum foot clearance F_C, the charts of $\log(E_{av})$, $\log(D_{av})$, $\log(T_L)$ and $\log(F_L)$ *vs.* (β, H_B) reveal significant changes. As can be observed in Fig. 9, $\log(E_{av})$, $\log(D_{av})$ and $\log(T_L)$ increase with β and decrease with H_B. The chart of F_L shows again a slightly different variation, being almost invariant for small values of β, while for higher values it decreases monotonically with β and H_B.

Figure 10 depicts the variation of the dynamic indices with the parameters L_S and F_C. The results are coherent since all indices decrease with L_S and increase with F_C. This variation is kept for different values of β and H_B.

From Figs. 8–10, it is concluded that the locomotion system should walk with the body on a relatively high position ($H_B \approx 0.9$ m), the steps should be long ($L_S \approx 3.0$ m) and the foot should remain near the ground ($F_C \approx 0$ m). Regarding the duty factor β, it is considered that it should be appropriate to use a small value for this parameter.

5.3. *Conclusions on the influence of parameters β, H_B, L_S and F_C*

In conclusion, the kinematic indices are in agreement with the dynamic indices. Therefore, it is possible to establish a compromise for optimising the WG, occurring the best situation for $\beta \approx 2\%$, $0.9 \leq H_B \leq 0.95$ m, $2.5 \leq L_S \leq 3.0$ m and $F_C \approx 0$ m, considering $L_{i1} = L_{i2} = 0.5$ m, $O_i = 0$ m and $V_F = 1$ ms^{-1} (it should be noticed that this value of β corresponds to the robot working on a running condition rather than just walking).

These results also seem to agree with several biological observations. In fact, regarding the optimal value of F_C, it should be referred that Neuhaus and Kazerooni (2000) developed a study of the human foot trajectory during the transfer phase based on some of Muybridge's photographic records and concluded that for different sorts of terrains, the

https://doi.org/10.1017/S0263574707003554 Published online by Cambridge University Press

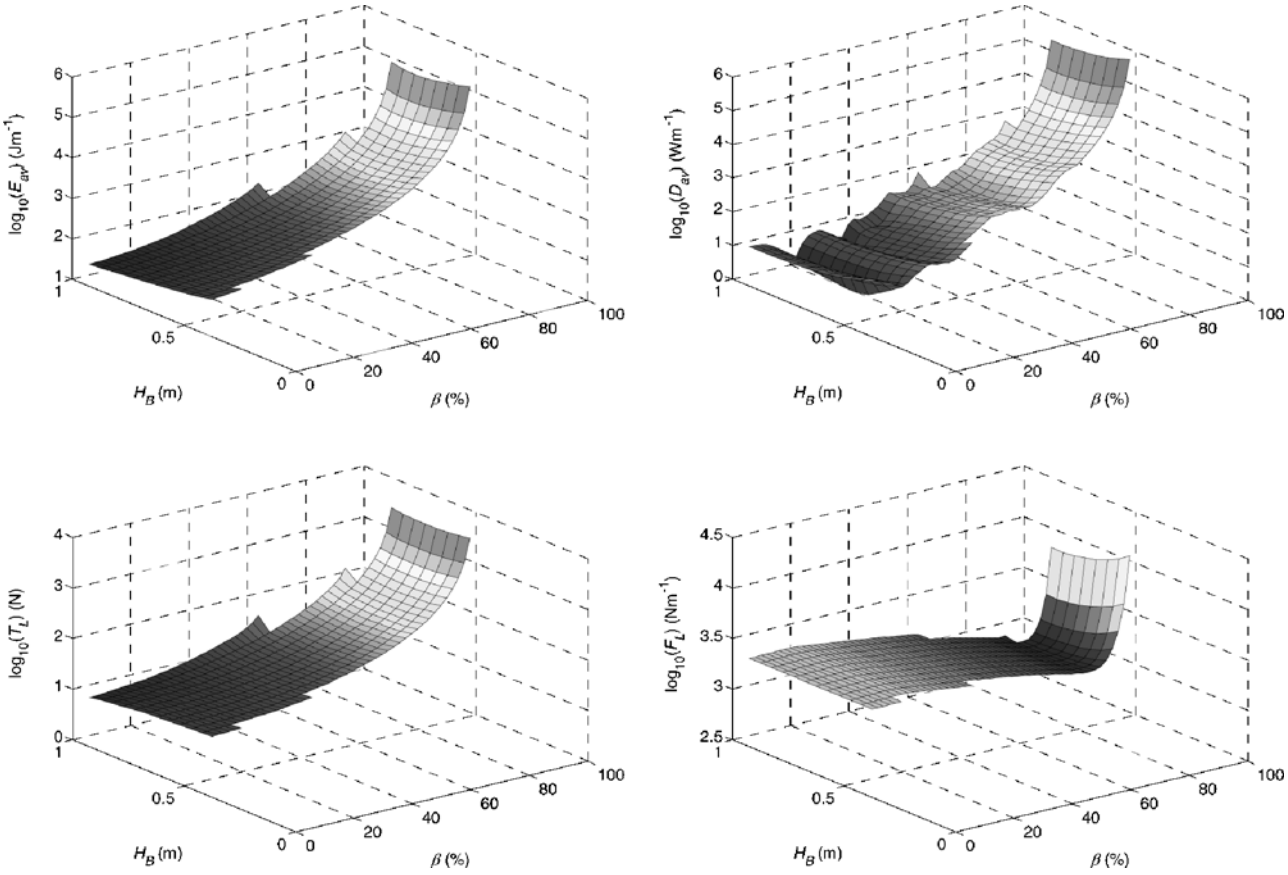


Fig. 8. Charts of $\log(E_{av})$, $\log(D_{av})$, $\log(T_L)$ and $\log(F_L)$ *vs.* (β, H_B) with $L_S = 1$ m, $F_C = 0.2$ m, WG.

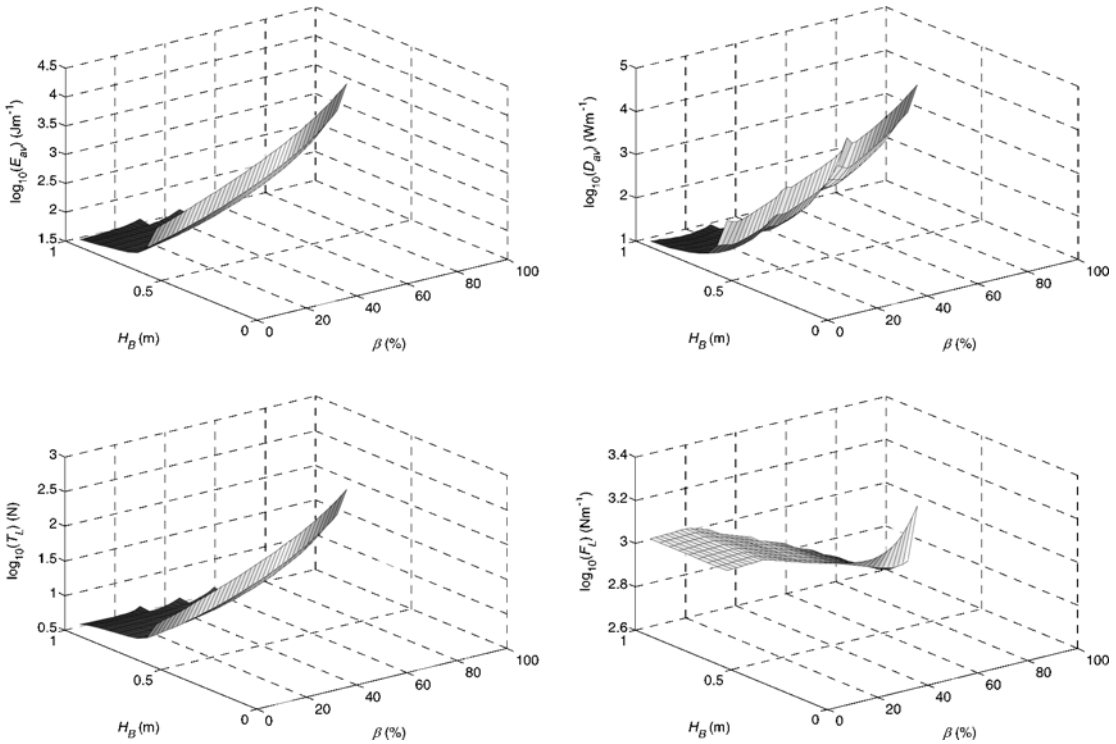


Fig. 9. Charts of $\log(E_{av})$, $\log(D_{av})$, $\log(T_L)$ and $\log(F_L)$ *vs.* (β, H_B) with $L_S = 2.0$ m, $F_C = 0.5$ m, WG.

https://doi.org/10.1017/S0263574707003554 Published online by Cambridge University Press

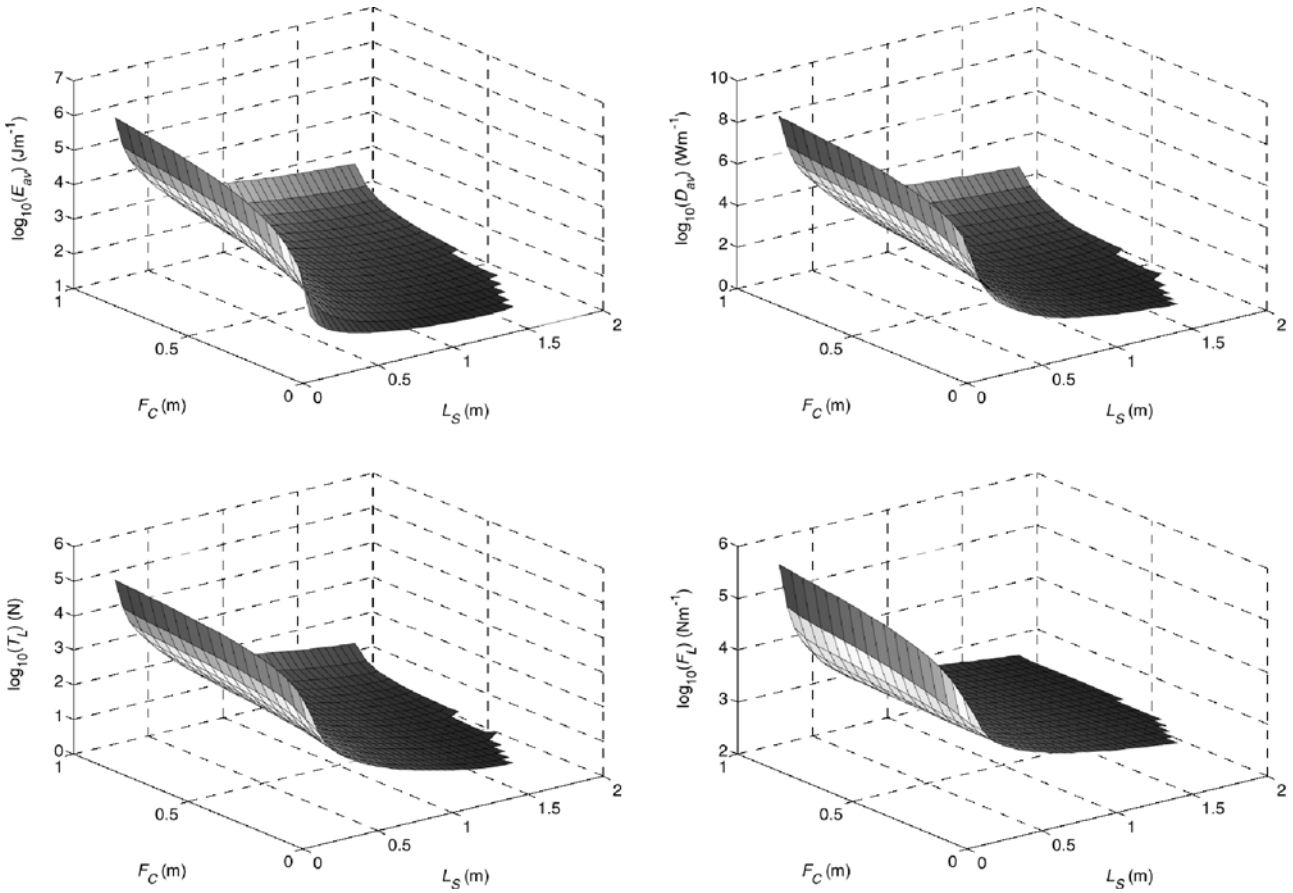


Fig. 10. Charts of $\log(E_{av})$, $\log(D_{av})$, $\log(T_L)$ and $\log(F_L)$ *vs.* (L_S, F_C) with $\beta = 50\%$, $H_B = 0.9$ m, WG.

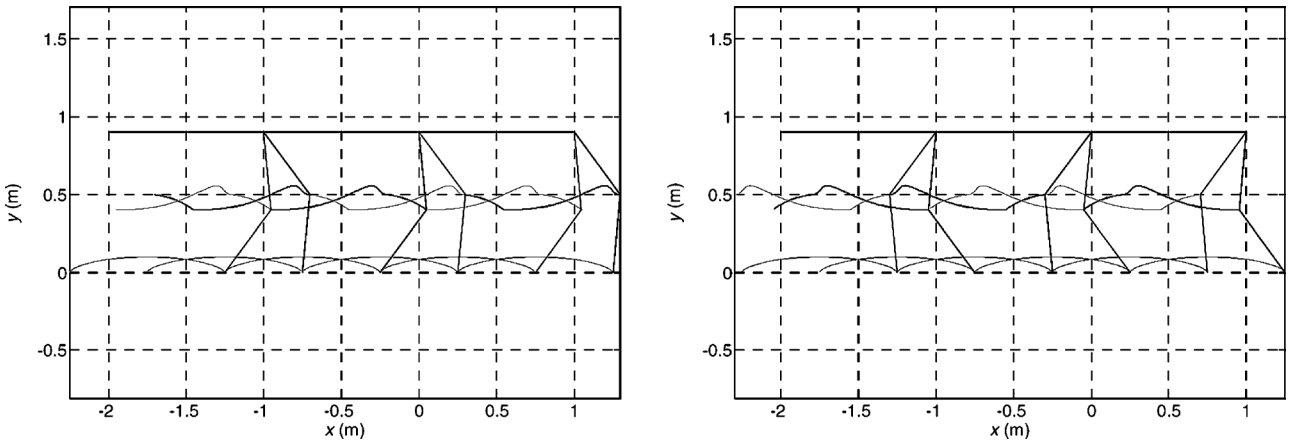


Fig. 11. Graphical representation of the robot locomotion in the situation where the legs present a structure similar to that of mammals (left) and that of the birds (right) with $\beta = 50\%$, $H_B = 0.9$ m, $L_S = 1.0$ m, $F_C = 0.1$ m, WG.

foot trajectories keep very close to the ground, irrespective of the gender of the human under study.

5.4. Leg configuration

In this section, a new set of experiments is performed for an alternative robot leg configuration. In the inverse kinematics, the solution corresponding to a backwards knee is selected in such a way that the hexapod robot presents legs similar to those of the flamingo (Fig. 11).

5.4.1. Kinematic analysis. This study starts again with the analysis of the kinematic indices variation *versus* the duty factor β and the body height H_B, for different values of the step length L_S and of the maximum foot clearance F_C. We observe a variation similar to the case in which the robot presents the front knee. However, in this case the perturbation indices present a relatively high value for small values of the body height. Similarly, for L_S and F_C it is concluded that the results are similar to those of the solution on which the robot presents the knee pointing to the front.

The variation of the locomobility indices with the duty factor and body height (Fig. 12) reveals that it is similar to the case of the mammal-type leg structure, for all values of the parameters L_S and F_C. Regarding their variation with

https://doi.org/10.1017/S0263574707003554 Published online by Cambridge University Press

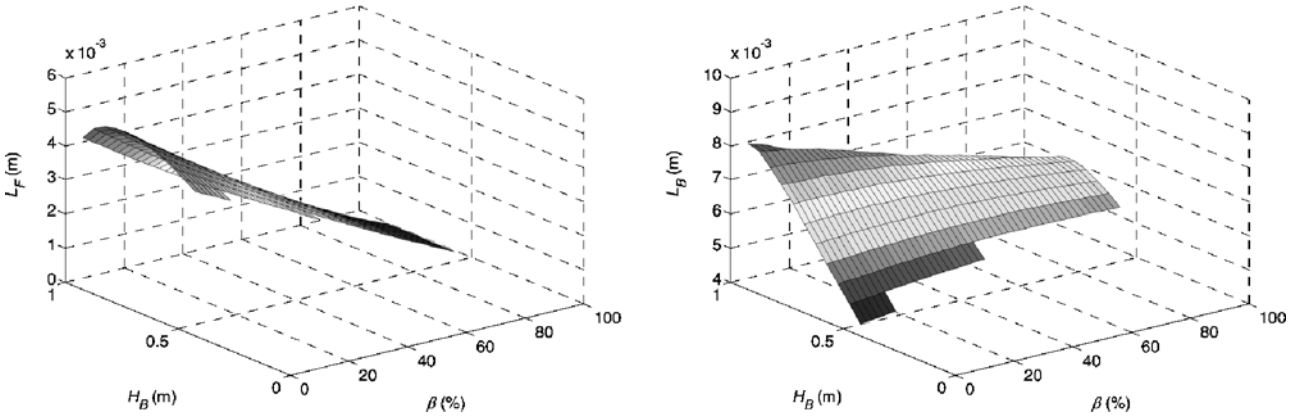


Fig. 12. Charts of L_F and L_B *vs.* (β, H_B) with $L_S = 1.0$ m, $F_C = 0.1$ m, WG.

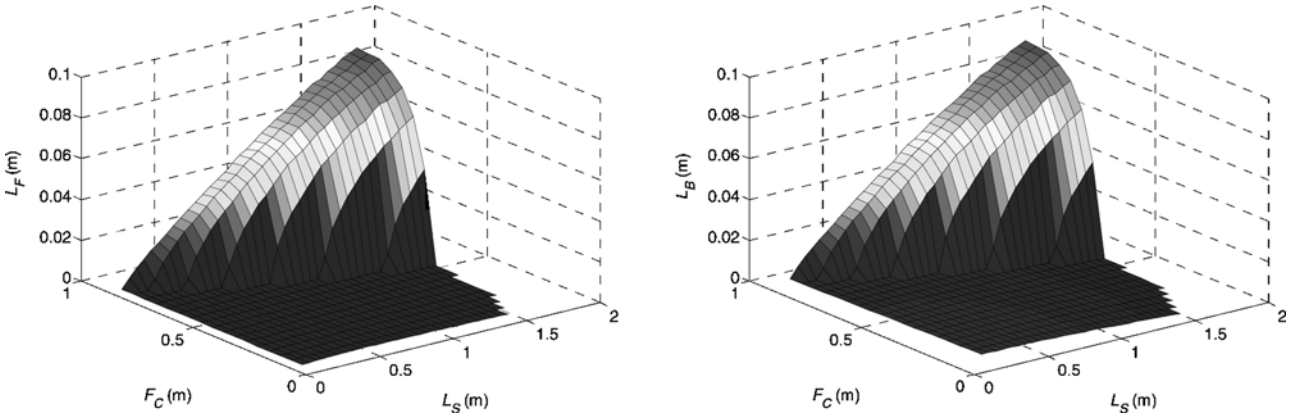


Fig. 13. Charts of L_F and L_B *vs.* (L_S, F_C) with $\beta = 50\%$, $H_B = 0.9$ m, WG.

L_S and F_C, Fig. 13 shows that they present the same sort of variation, namely that they increase with F_C and L_S. This pattern is kept for different values of β and H_B. This is the main difference when compared to the situation where the leg presents the mammals structure. According with the locomobility indices it is preferable to move with a high value of F_c.

The analysis developed here is repeated in the following subsection from the viewpoint of the dynamic indices.

5.4.2. Dynamic analysis. Figure 14 depicts the charts of $\log(E_{av})$, $\log(D_{av})$, $\log(T_L)$ and $\log(F_L)$ *vs.* (β, H_B). It is concluded that the indices present a shape similar to those in the situation in which the robot presents the legs with a mammal structure. The charts of $\log(E_{av})$, $\log(D_{av})$ and $\log(T_L)$ increase monotonically with β and decrease slightly with H_B. Moreover, the chart of $\log(D_{av})$ has the particularity of showing a minimum at $\beta = 16\%$ and $H_B = 0.9$ m, as observed previously. Finally, the index F_L also presents a slightly different variation, being almost invariant with the parameter H_B, except for high values of β where it decreases slightly. Concerning its variation with the duty factor, the chart presents a minimum at $\beta \approx 88\%$.

The variation of the dynamic indices with L_S and F_C is shown in Fig. 15. The results are coherent since all indices decrease with L_S and increase with F_C, and the variation remains for different values of β and H_B. Comparing these charts with those of Fig. 10 (for the situation on which the robot presents the mammal leg structure) it is concluded that they are nearly identical.

Figures 14 and 15 show that the artificial locomotion system should walk with the body on a relatively high position, the steps should be long and the foot should remain near the ground. Regarding the duty factor, since the index F_L is the only one that points out for the use of a high value, it is considered that it is adequate to use a reduced value of this parameter.

In conclusion, the experiments completed in this section are not conclusive in what concerns the best knee position in relation to the hip.

5.5. Locomotion gaits

The study is now extended for the different periodic gaits considered, namely the EPHCG, EPFCG, BWG, BEPHCG and BEPFCG. With this objective in mind, the simulations of Sections 5.1 and 5.2 are repeated for all these gaits and the results are analysed.

5.5.1. Kinematic analysis. For the kinematic indices, the charts do not vary significantly with the adopted gait. In other words, the performance variation with the parameters β, H_B, L_S and F_C is similar for all considered periodic gaits.

For example, Fig. 16 presents the charts of L_F for the gaits under consideration. Comparing all charts it is verified that they are identical, presenting a maximum at $L_S = 0.75$ m

https://doi.org/10.1017/S0263574707003554 Published online by Cambridge University Press

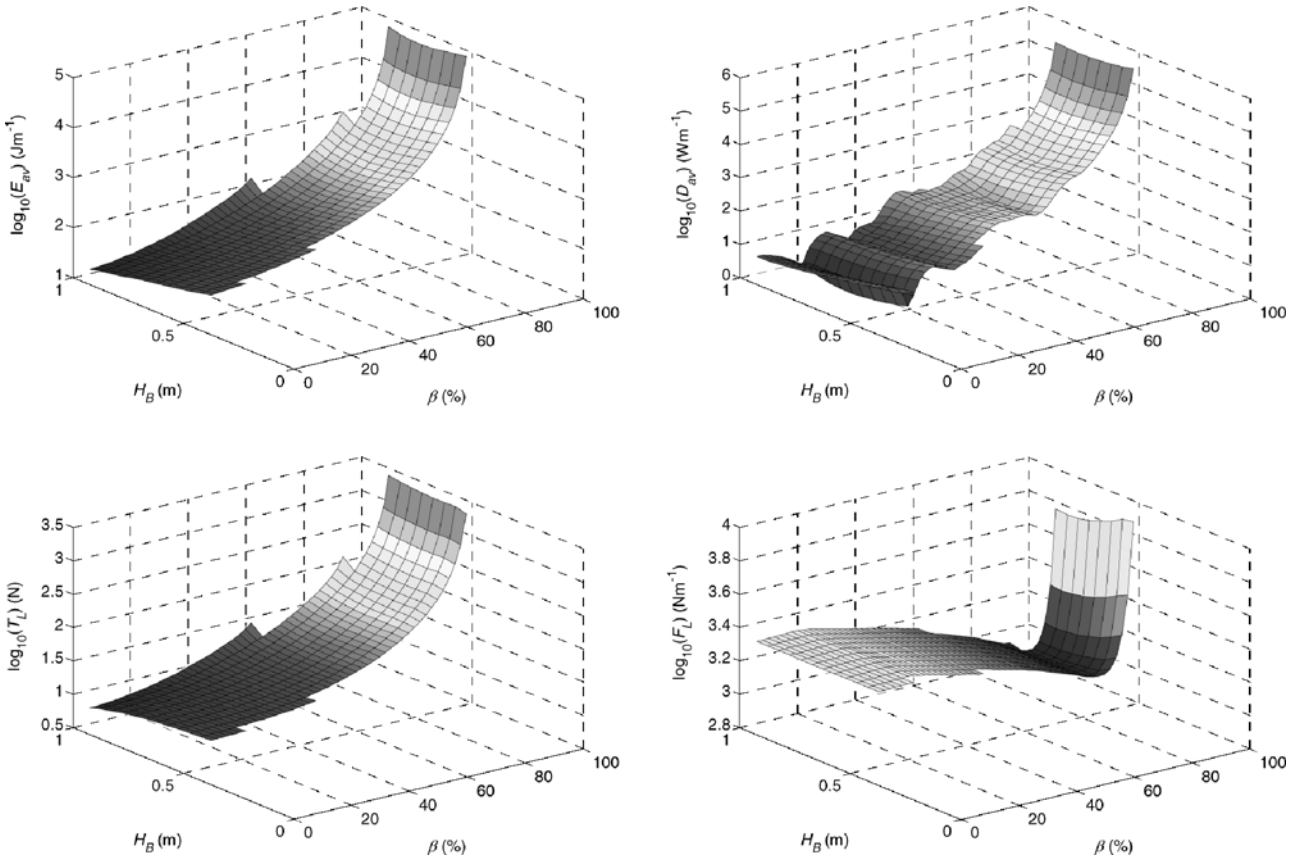


Fig. 14. Charts of $\log(E_{av})$, $\log(D_{av})$, $\log(T_L)$ and $\log(F_L)$ *vs.* (β, H_B) with $L_S = 1.0$ m, $F_C = 0.1$ m, WG.

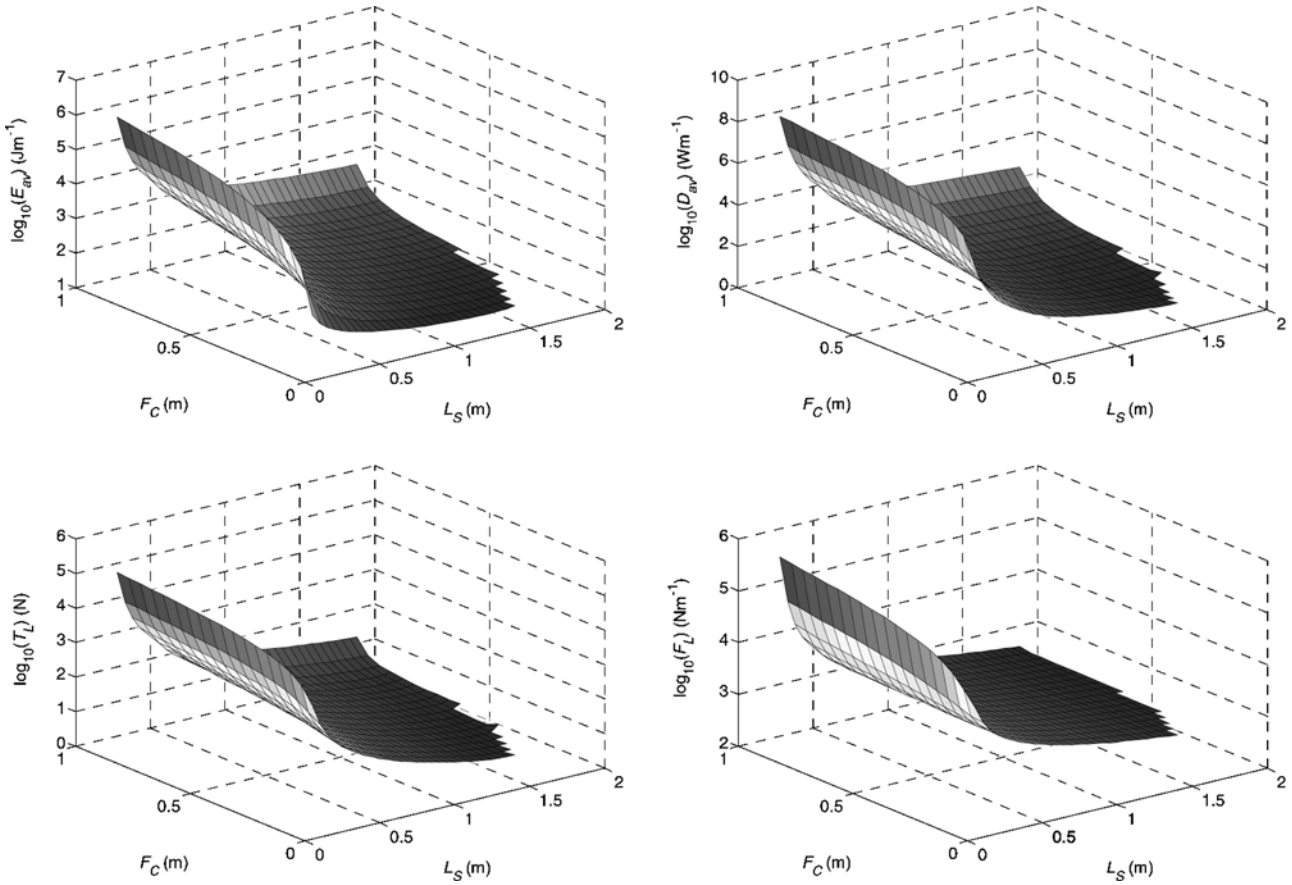


Fig. 15. Charts of $\log(E_{av})$, $\log(D_{av})$, $\log(T_L)$ and $\log(F_L)$ *vs.* (L_S, F_C) with $\beta = 50\%$, $H_B = 0.9$ m, WG.

https://doi.org/10.1017/S0263574707003554 Published online by Cambridge University Press

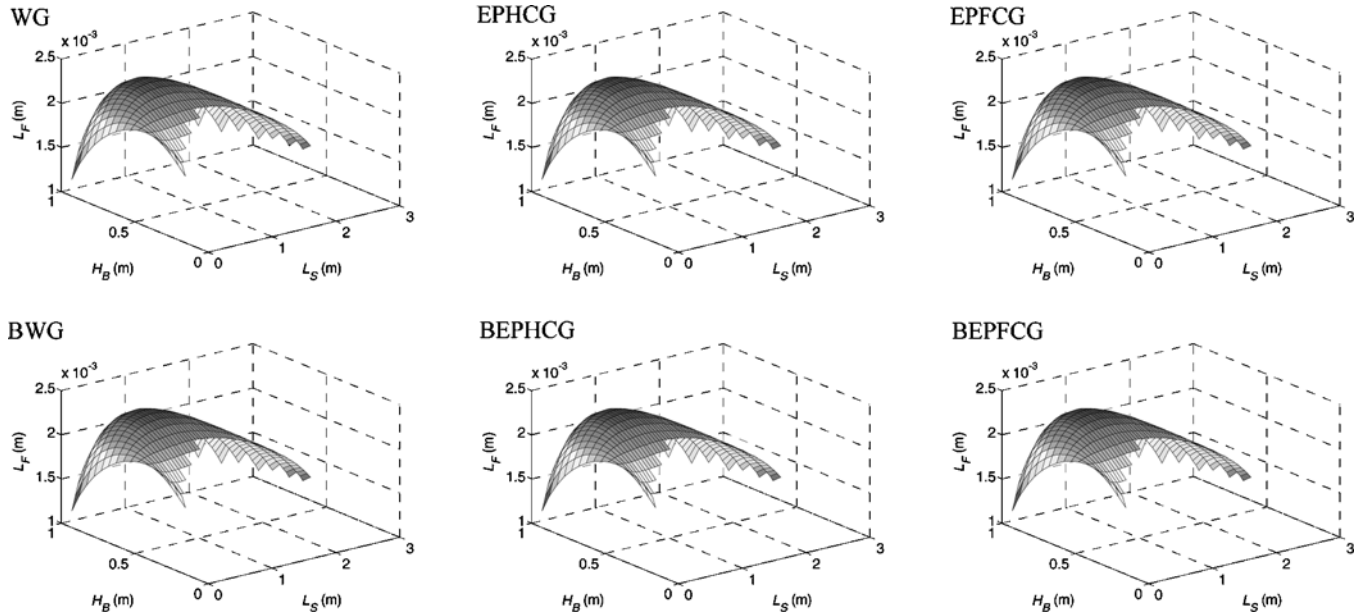


Fig. 16. Charts of L_F *vs.* (L_S, H_B) with $\beta = 50\%$, $F_C = 0.1$ m, WG, EPHCG, EPFCG, BWG, BEPHCG and BEPFCG.

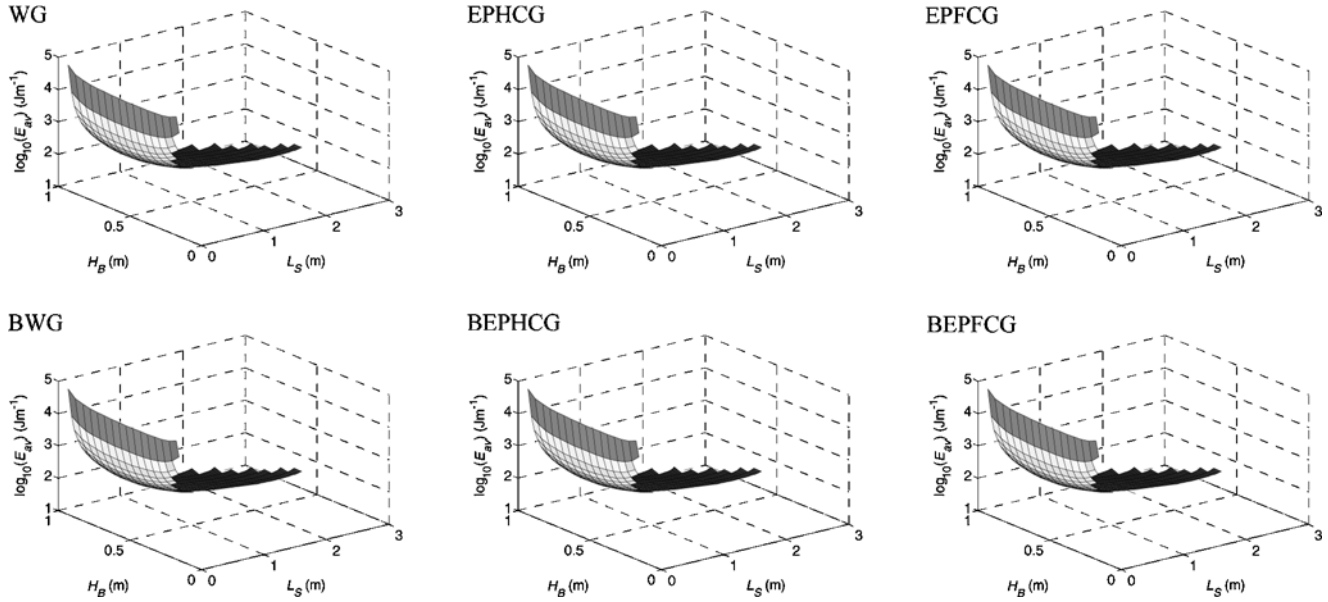


Fig. 17. Charts of $\log(E_{av})$ *vs.* (L_S, H_B) with $\beta = 50\%$, $F_C = 0.1$ m, $V_F = 1$ ms^{-1}, WG, EPHCG, EPFCG, BWG, BEPHCG and BEPFCG.

and $H_B = 0.75$ m, and that the influence of the different parameters is identical for the different gaits.

5.5.2. Dynamic analysis. For the dynamical indices, the charts do not vary significantly with the adopted gait. Furthermore, it is observed (Fig. 17) that the variation of the dynamic indices with β, H_B, L_S and F_C is similar. Therefore, a complementary analysis (and the definition of an adequate index) is needed in order to compare the performance of the distinct periodic walking gaits.

5.5.3. Instantaneous absolute mechanical power versus gait. In this section, the gait performance is evaluated through the total instantaneous absolute mechanical power $P_t(t)$ (Eq. 7b) along one period of the robot locomotion cycle, for several periodic gaits.

Figures 18–20 present the charts of $P_t(t)$ for different values of β. It is concluded that $P_t(t)$ increases with β and that the EPHCG and the EPFCG require smaller peaks of $P_t(t)$ than the WG. This result should be expected since, with the increase of the duty factor, the robot has less time to execute the leg transfer and, therefore, needs to move it with a higher velocity consequently increasing the energy consumption. Moreover, for two particular values of the duty factor, namely for $\beta = 33.3\%$ and $\beta = 66.6\%$, it is verified that all studied locomotion gaits present identical curves of $P_t(t)$.

For the backward gaits (BWG, BEPHCG and BEPFCG), the evolution of $P_t(t)$ is similar to the one that occurs for the forward gaits. Therefore, we conclude that the WG is less efficient than EPHCW and EPFCW from the viewpoint of an autonomous energy source.

https://doi.org/10.1017/S0263574707003554 Published online by Cambridge University Press

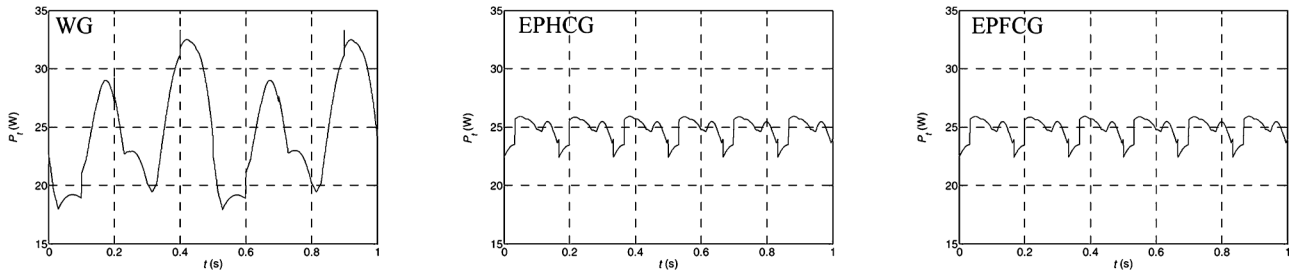


Fig. 18. Charts of $P_t(t)$ with $\beta = 20.0\%$, $H_B = 0.9$ m, $L_S = 1.0$ m, $F_C = 0.1$ m and $V_F = 1$ ms^{-1}, for the WG, EPHCG and EPFCG.

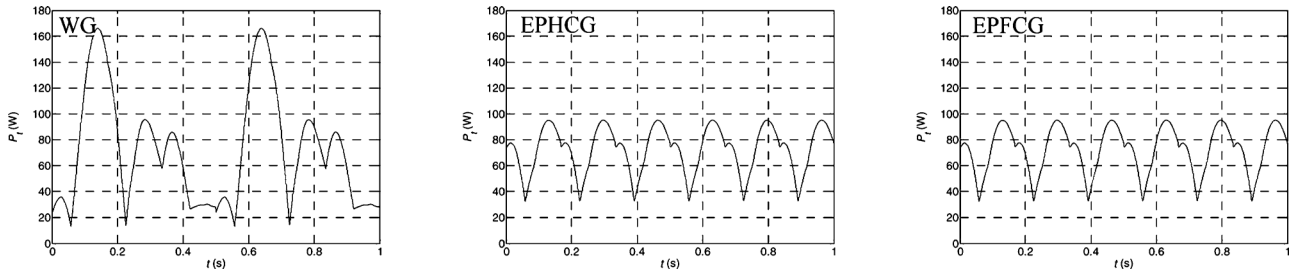


Fig. 19. Charts of $P_t(t)$ with $\beta = 50.0\%$, $H_B = 0.9$ m, $L_S = 1.0$ m, $F_C = 0.1$ m and $V_F = 1$ ms^{-1}, for the WG, EPHCG and EPFCG.

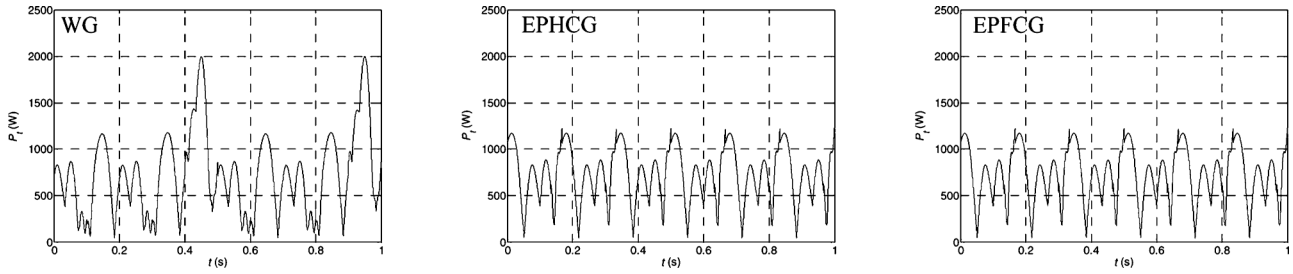


Fig. 20. Charts of $P_t(t)$ with $\beta = 80.0\%$, $H_B = 0.9$ m, $L_S = 1.0$ m, $F_C = 0.1$ m and $V_F = 1$ ms^{-1}, for the WG, EPHCG and EPFCG.

Summing the instantaneous absolute mechanical power for the legs of the left and right sides of the robot, i.e. $P_{\text{left}}(t) = P_1(t) + P_3(t) + P_5(t)$ and $P_{\text{right}}(t) = P_2(t) + P_4(t) + P_6(t)$, respectively, we conclude that all gaits pose similar requirements, but the EPFCG presents lower consumption peaks. This situation is clear for $\beta < 60.0\%$ (Fig. 21). For higher values of β, it is verified that $P_{\text{left}}(t)$ and $P_{\text{right}}(t)$ are approximately identical for the different gaits under study, the EPHCG being the gait that demands higher peaks. Moreover, from this viewpoint the forward and backward gaits pose similar requirements.

Finally, the sums of the instantaneous absolute mechanical power for the front, middle and rear legs of the hexapod robot are compared, i.e. $P_{\text{front}}(t) = P_1(t) + P_2(t)$, $P_{\text{middle}}(t) = P_3(t) + P_4(t)$ and $P_{\text{rear}}(t) = P_5(t) + P_6(t)$, respectively. In this perspective, there is not any difference between the locomotion gaits since they present similar curves having only a different phase. This result is expected since the legs perform the same trajectory, the locomotion gaits under study are symmetrical and, therefore, with a half cycle phase difference between the legs on each side of the robot body.

5.6. *Foot trajectory offset versus legs links length*

In the previous experiments, the links lengths and the masses of the robot legs were maintained constant with the values $L_{i1} = L_{i2} = 0.5$ m and $M_{i1} = M_{i2} = 1.0$ kg for $O_i = 0.0$ m.

In this section, the influence of these parameters upon the kinematic and dynamic indices is studied. Therefore, the relation between the two links is varied making $M_{ij} = (L_{ij}/L_{it})M_{Lit}$ $(i = 1, \ldots, 6; j = 1, 2)$, while a constant total length and mass of the legs are established that are equal to $L_{it} = L_{i1} + L_{i2} = 1.0$ m and $M_{Lit} = M_{i1} + M_{i2} = 2.0$ kg.

5.6.1. Kinematic analysis. With these ideas in mind, we start by analysing the behaviour of the perturbation analysis, $\xi_{\dot{x}}$ and $\xi_{\dot{y}}$, for different values of the locomotion parameters. Regarding $\xi_{\dot{x}}$, it is verified (Fig. 22) that, for small values of H_B and L_S, it is preferable to have robot legs with small values of L_{i1} and walking trajectories with the feet shifted backwards relatively to the hips ($O_i < -0.5$ m). From the viewpoint of $\xi_{\dot{y}}$, the robot should have legs with identical values of L_{i1} and L_{i2}, and should walk with the feet aligned with the hips ($O_i \approx 0.0$ m).

As H_B increases, $\xi_{\dot{x}}$ (Fig. 23) indicates an optimum robot with high values of L_{i1} and a locomotion with feet shifted backwards relatively to the hips ($O_i < -0.5$ m). Regarding $\xi_{\dot{y}}$, its behaviour is kept as described previously.

Performing a similar analysis with the locomobility indices L_F and L_B, it is concluded that the results are

https://doi.org/10.1017/S0263574707003554 Published online by Cambridge University Press

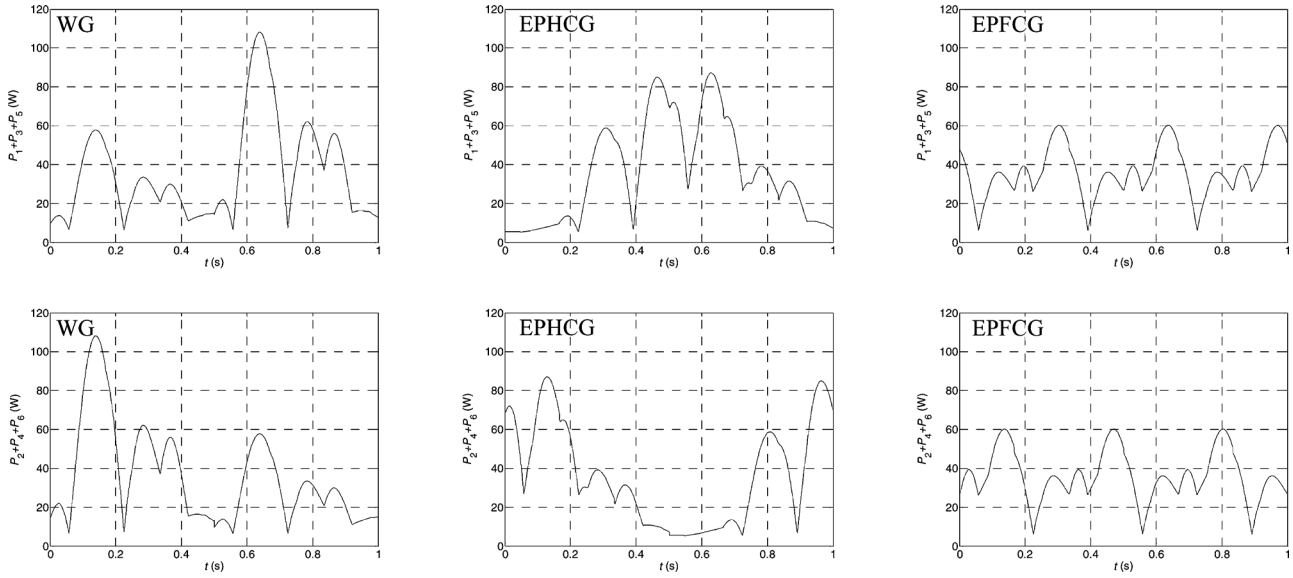


Fig. 21. Charts of the sums of the instantaneous absolute mechanical power of the left ($P_1(t) + P_3(t) + P_5(t)$) and right ($P_2(t) + P_4(t) + P_6(t)$) sides of the robot for $\beta = 50\%$, $H_B = 0.9$ m, $L_S = 1.0$ m, $F_C = 0.1$ m and $V_F = 1$ ms^{-1}, for the WG, EPHCG and EPFCG.

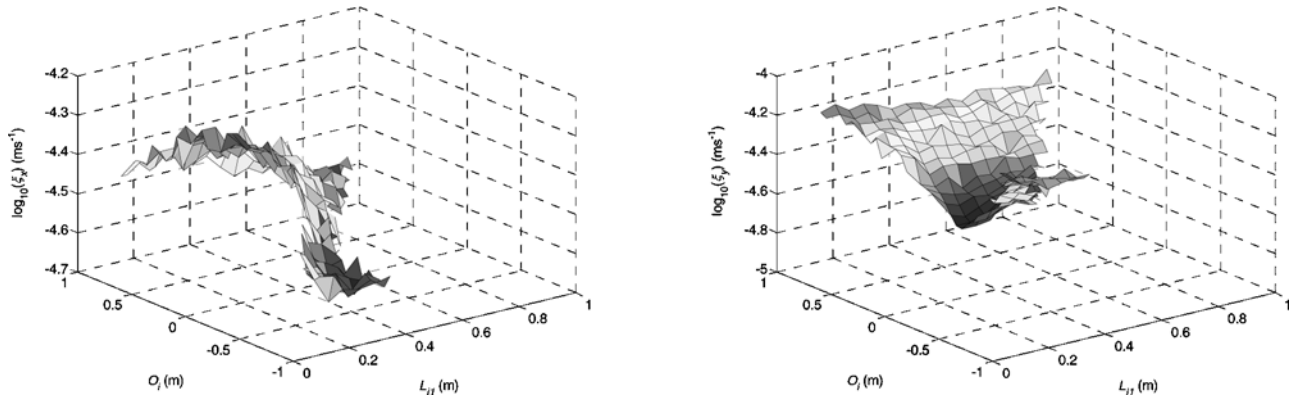


Fig. 22. Charts of $\log(\xi_{\dot{x}})$ and $\log(\xi_{\dot{y}})$ *vs.* (L_{i1}, O_i) with $\beta = 50\%$, $L_S = 0.2$ m, $H_B = 0.4$ m, $F_C = 0.1$ m, WG.

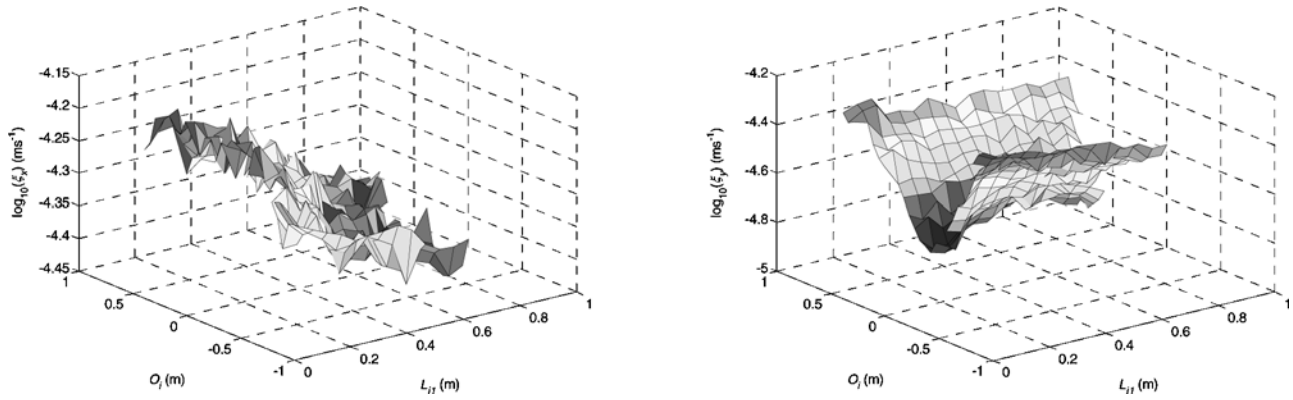


Fig. 23. Charts of $\log(\xi_{\dot{x}})$ and $\log(\xi_{\dot{y}})$ *vs.* (L_{i1}, O_i) with $\beta = 50\%$, $L_S = 0.2$ m, $H_B = 0.7$ m, $F_C = 0.1$ m, WG.

consistent (Fig. 24). It is verified that $L_F(L_{i1}, O_i)$ and $L_B(L_{i1}, O_i)$ present maximum values for legs links lengths $L_{i1} \approx 0.5$ m and a foot trajectory offset $O_i \approx 0.0$ m. Besides, it is also possible to conclude that L_F and L_B decrease sharply/slightly for values of L_{i1}/O_i far from these. The results (Fig. 25) are also invariant with the different locomotion parameters, except in the case when the body height is kept at a small value. In this situation, it is verified that the maximum values of L_F and L_B are kept near $L_{i1} \approx 0.5$ m but, in accordance with the index L_F, the robot foot trajectory must be shifted to the front or to the back relatively to the hip ($O_i \neq 0.0$ m).

5.6.2. Dynamic analysis. In this section, the influence of L_{i1} and O_i is analysed in the perspective of the dynamic indices. It is concluded that the charts (Fig. 26) of $\log(E_{av})$, $\log(D_{av})$

https://doi.org/10.1017/S0263574707003554 Published online by Cambridge University Press

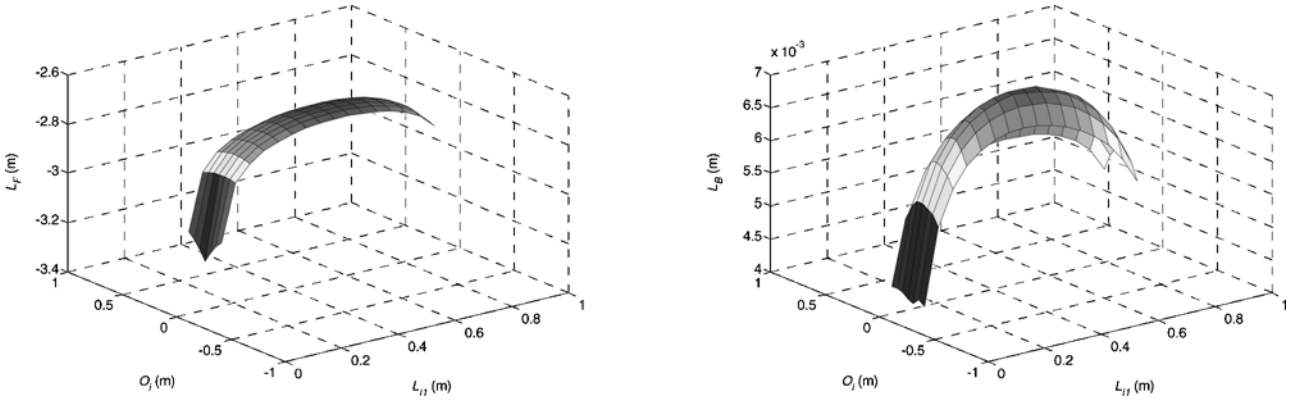


Fig. 24. Charts of L_F and L_B *vs.* (L_{i1}, O_i) with $\beta = 50\%$, $L_S = 1.0$ m, $F_C = 0.1$ m, $H_B = 0.9$ m, $V_F = 1$ ms^{-1}, WG.

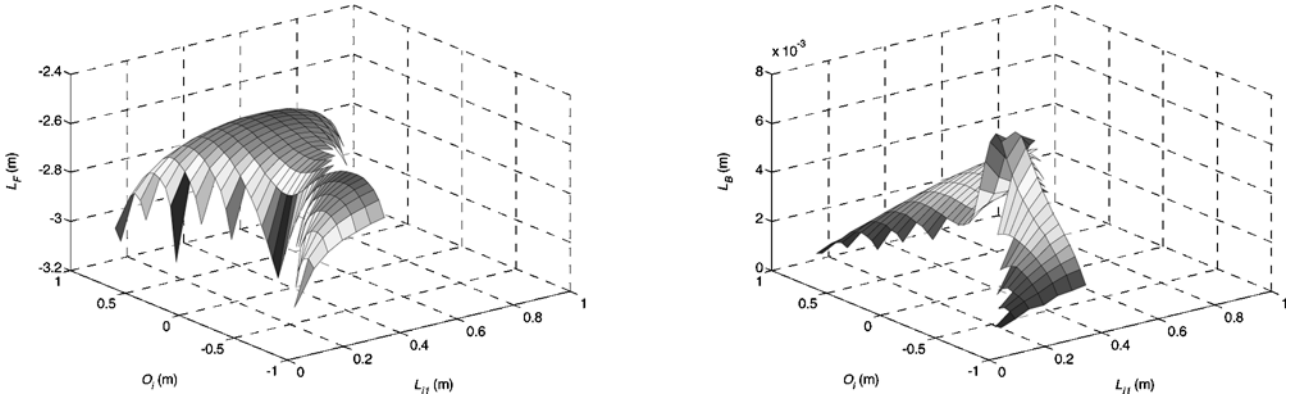


Fig. 25. Charts of L_F and L_B *vs.* (L_{i1}, O_i) with $\beta = 50\%$, $L_S = 0.2$ m, $F_C = 0.1$ m, $H_B = 0.4$ m, $V_F = 1$ ms^{-1}, WG.

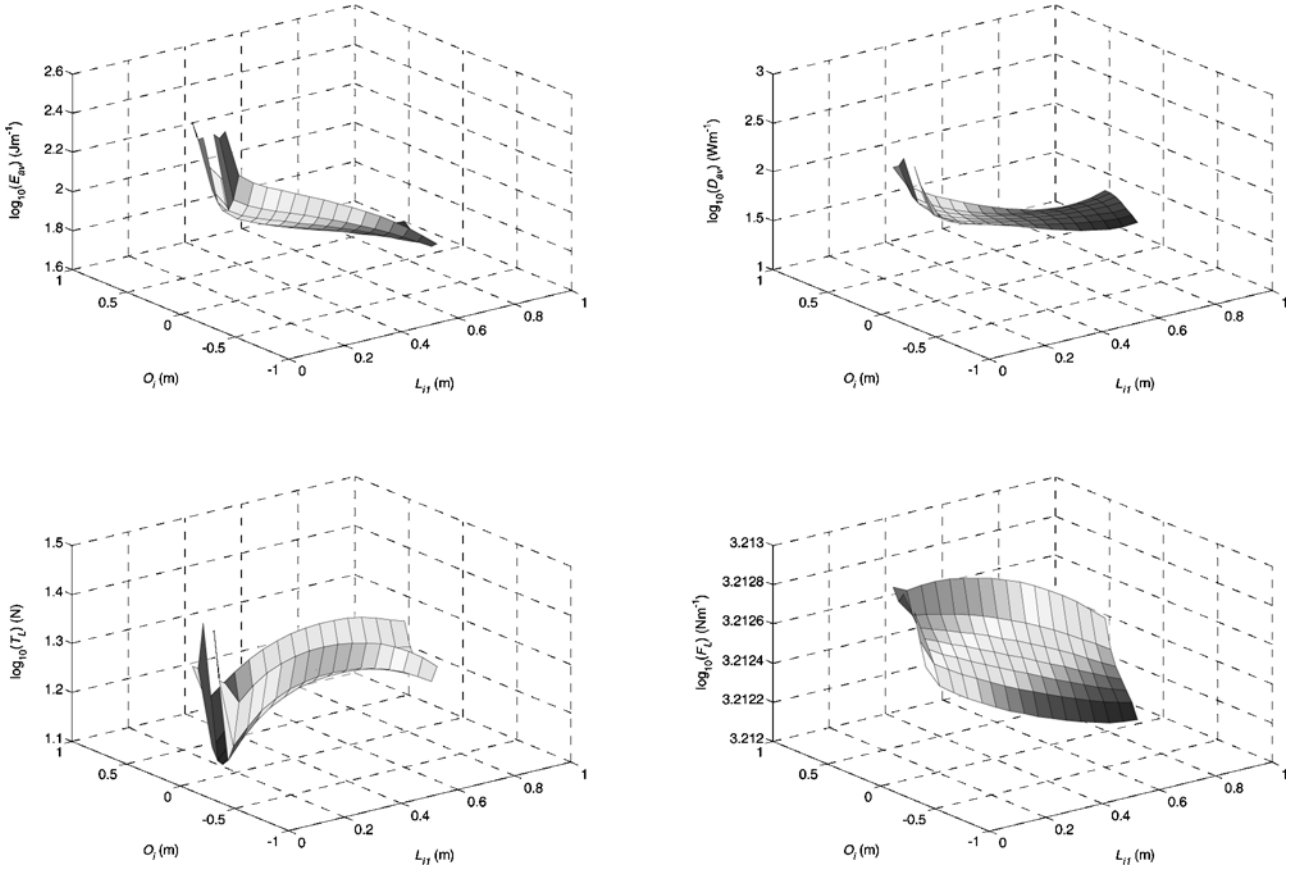


Fig. 26. Charts of $\log(E_{av})$, $\log(D_{av})$, $\log(T_L)$ and $\log(F_L)$ *vs.* (L_{i1}, O_i) with $\beta = 50\%$, $L_S = 1.0$ m, $F_C = 0.1$ m, $H_B = 0.9$ m, $V_F = 1$ ms^{-1}, WG.

https://doi.org/10.1017/S0263574707003554 Published online by Cambridge University Press

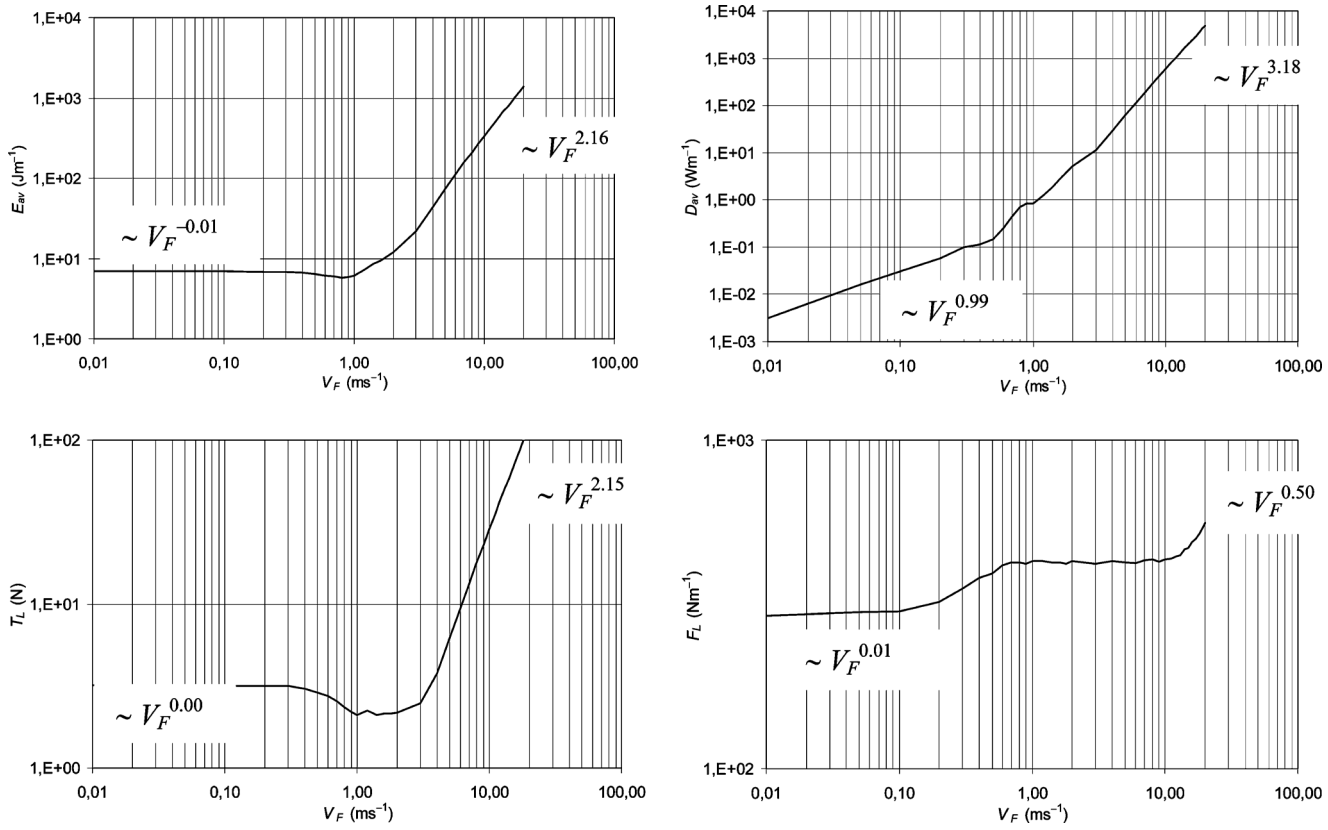


Fig. 27. Charts of min$[E_{av}(V_F)]$, min$[D_{av}(V_F)]$, min$[T_L(V_F)]$ and min$[F_L(V_F)]$ with $F_C = 0.01$ m, WG.

and log(T_L) present similar behaviours in what respects their variation with O_i (all present minimum values when the locomotion is performed with $O_i \approx 0.0$ m). However, in what concerns their variation with L_{i1}, the results are contradictory. According to E_{av}, the locomotion should be performed with values near the maximum while in the perspective of D_{av}, it should have values near $L_{i1} \approx 0.7$ m, and in the viewpoint of T_L, it should have small values. The index F_L presents a monotonic variation in the entire range indicating an optimal locomotion with the minimum/maximum values of O_i/L_{i1}, respectively. It is confirmed that these results are invariant with the distinct parameters under study (β, H_B, L_S and F_C). Therefore, a compromise of the different indices indicates that the locomotion should be performed with $L_{i1} \approx 0.5$ m and $O_i \approx 0.0$ m.

The analysis is extended for a new case in which the masses of the legs segments remain constant (contrarily to the previous case in which the masses are varied proportionally to the segment length). Therefore, a total constant length and mass such that $L_{it} = L_{i1} + L_{i2} = 1.0$ m and $M_{Lit} = M_{i1} + M_{i2} = 2.0$ kg are established, while the relation between the two links is varied according to $M_{ij} = 1.0$ kg ($i = 1, \ldots, 6$; $j = 1, 2$).

The charts of log(E_{av}), log(D_{av}) and log(T_L) reveal similar variations, and we conclude that the locomotion is more efficient for $L_{i1} \approx 0.2$ m and $O_i \approx 0.0$ m. As in the previous case, F_L presents a monotonic variation in all range of values, indicating an optimum locomotion performed with the minimum/maximum values of O_i/L_{i1}, respectively.

Again it is observed that the results do not change with β, H_B, L_S and F_C. Therefore, we conclude that it is possible to establish a compromise between the different perspectives according to which the locomotion should be performed with $L_{i1} \approx 0.2$ m and $O_i \approx 0.0$ m.

These results seem to agree with the biology, particularly with the mammals, because it is verified that these animals have legs with links of approximately the same length (Witte *et al.*, 2001a). Moreover, the last results are also in agreement with biological studies by Kram *et al.* (1997) pointing that the leg mass must be concentrated as close as possible to the hip.

5.7. *Robot body forward velocity*

After having determined the optimal values for the parameters of the robot structure and gait, the effect of other parameters may be studied. In particular, it is important to investigate the effect of the travelling velocity V_F since the parameters seem to have a large influence (Cham *et al.*, 2002).

With this objective in mind, a set of experiments is performed with the objective of determining the minimal values of the dynamic indices for different velocities, while the corresponding values of β, H_B and L_S are captured. During the experiments, the value of F_C is kept constant ($F_C = 0.01$ m) since the previous results pointed this to be the optimal value.

Figure 27 shows the evolution of min$[E_{av}(V_F)]$, min$[D_{av}(V_F)]$, min$[T_L(V_F)]$ and min$[F_L(V_F)]$. This figure reveals that min$[E_{av}]$ increases with V_F, being min$[E_{av}] \sim V_F^{-0.01}$ for low velocities and min$[E_{av}] \sim V_F^{2.16}$ for high velocities. This chart presents a transition in the range $0.4 < V_F < 3.0$ ms^{-1} with a minimum at $V_F \approx 0.8$ ms^{-1}.

https://doi.org/10.1017/S0263574707003554 Published online by Cambridge University Press

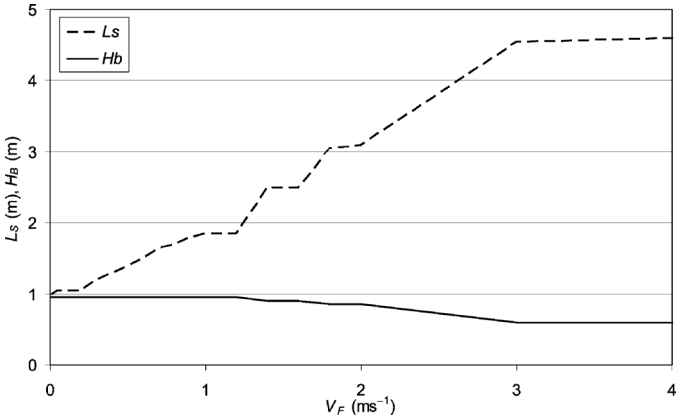


Fig. 28. Chart of $L_S(V_F)$ and $H_B(V_F)$ for the minimal values of E_{av}, $F_C = 0.01$ m, WG.

The chart of $\min[D_{av}]$ presents a similar variation: $\min[D_{av}] \sim V_F^{0.99}$ for low velocities and $\min[D_{av}] \sim V_F^{3.18}$ for high velocities. The chart presents a transition in the range $0.2 < V_F < 3.0$ ms^{-1}.

The evolution of $\min[T_L]$ also has $\min[T_L] \sim V_F^{0.00}$ for low velocities and $\min[T_L] \sim V_F^{2.15}$ for high velocities. The transition occurs in the range $0.3 < V_F < 4.0$ ms^{-1} and, in this case, we have a minimum for $V_F \approx 1.0$ ms^{-1}.

The chart of $\min[F_L]$ is slightly different with two distinct levels. Additionally, we have $\min[F_L] \sim V_F^{0.01}$ for low velocities and $\min[F_L] \sim V_F^{0.50}$ for high velocities. The transitions from low to medium and medium to high velocities occur for $V_F \approx 0.3$ ms^{-1} and $V_F \approx 10.0$ ms^{-1}, respectively.

The main conclusion retrieved from Fig. 27 is that the minimum values of E_{av}, D_{av} and T_L have a slight variation in the range $0.01 < V_F < 2.0$ ms^{-1}, after which they increase rapidly. Therefore, the locomotion executed within this velocity range presents almost a constant performance. However, with the robot geometry under consideration, if the machine is required to move at higher velocities then its performance suffers a dramatic degradation. Furthermore, it is verified that the locomotion is very efficient when executed at velocities in the range $0.8 < V_F < 1.0$ ms^{-1}.

5.8. Body height and step length versus robot body forward velocity

Figure 28 shows the evolution of $L_S(V_F)$ and $H_B(V_F)$ for the minimum values of E_{av}. It is possible to conclude that for $V_F \leq 3$ ms^{-1}, the index L_S (H_B) increases (decreases) with V_F from $L_S = 1.0$ m ($H_B = 0.95$ m) up to $L_S = 4.5$ m ($H_B = 0.6$ m). Other charts reveal that $L_S(V_F)$ and $H_B(V_F)$ present the same variation for the minimum values of the indices D_{av}, T_L and F_L.

These results complement the previous conclusions presented in Sections 5.1 and 5.2, concerning the choice of the locomotion parameters in order to optimise the locomotion. They show clearly that the step length and the body height should be adapted to the robot locomotion velocity.

Regarding the duty factor value, it is verified that for the range of velocities under study and independently of the dynamic index, it should remain close to a small value ($\beta \approx 2\%$). This means that the optimum situation, from the viewpoint of overall indices, corresponds to a running robot ($\beta < 50\%$).

5.9. Number of robot legs

The studies performed up to this point were based on a hexapod artificial locomotion system. Now we try to find out whether there is an optimum number of robot legs (n) that should be adopted for locomotion as a function of velocity V_F. For this purpose, two alternatives are considered.

The first option is to establish that each leg mass is constant and, as a result, the total robot mass (M_{Rt}) varies with the total number of legs (n)

$$M_{Rt} = M_b + \sum_{i=1}^{n}(M_{i1} + M_{i2}), \quad M_{i1} = M_{i2} = 1.0 \text{ kg} \qquad (11)$$

where M_b is the mass of the body.

Figure 29 shows that E_{av} increases proportionally with n. For the index T_L we get similar conclusions, whereas D_{av} and F_L increase with n only for high values of V_F.

From the viewpoint of E_{av} and T_L, the most efficient way to perform the locomotion independently of V_F is to adopt biped robots while, on the opposite side, robots with ten legs are the most inefficient. The results obtained trough the indices D_{av} and F_L point out in the direction of the existence of velocities ranges where each of the structures is more efficient.

The second alternative for the comparison is to consider that the total robot mass (M_{Rt}) is constant

$$M_{Rt} = M_b + \sum_{i=1}^{n}(M_{i1} + M_{i2}), \quad M_{Rt} = 100.0 \text{ kg} \qquad (12)$$

In this case, the mass of the legs varies with n according to the expression (Taylor *et al.*, 1982; Fedak *et al.*, 1982; Heglund *et al.*, 1982)

$$\frac{(M_{i1} + M_{i2})}{M_{Rt}} = 0.35e^{-0.47n}, \; M_{i1} = M_{i2}, \; \forall i \qquad (13)$$

Figure 30 shows that E_{av} decreases proportionally with n. As can be seen, the indices D_{av} and T_L present a similar variation to E_{av}. The index F_L reveals a more complex variation, pointing out that the different structures present optimal efficiencies at different velocity ranges.

These last results are in accordance with the biology studies developed by Kram *et al.* (1997). When animals move at relatively high velocities, the smaller the mass of the legs the smaller is the kinetic energy spent, because they need to move the legs at a high frequency.

Comparing these last experiments, a compromise for optimising the WG must be established. Therefore, the robot should walk (in fact it should "run," due to $\beta < 50\%$) with a velocity $V_F \approx 1$ ms^{-1}, and the robot mass must be concentrated on the body, the legs should be as light as possible. If all legs have the same mass, one should choose the locomotion system with the lower number of legs.

https://doi.org/10.1017/S0263574707003554 Published online by Cambridge University Press

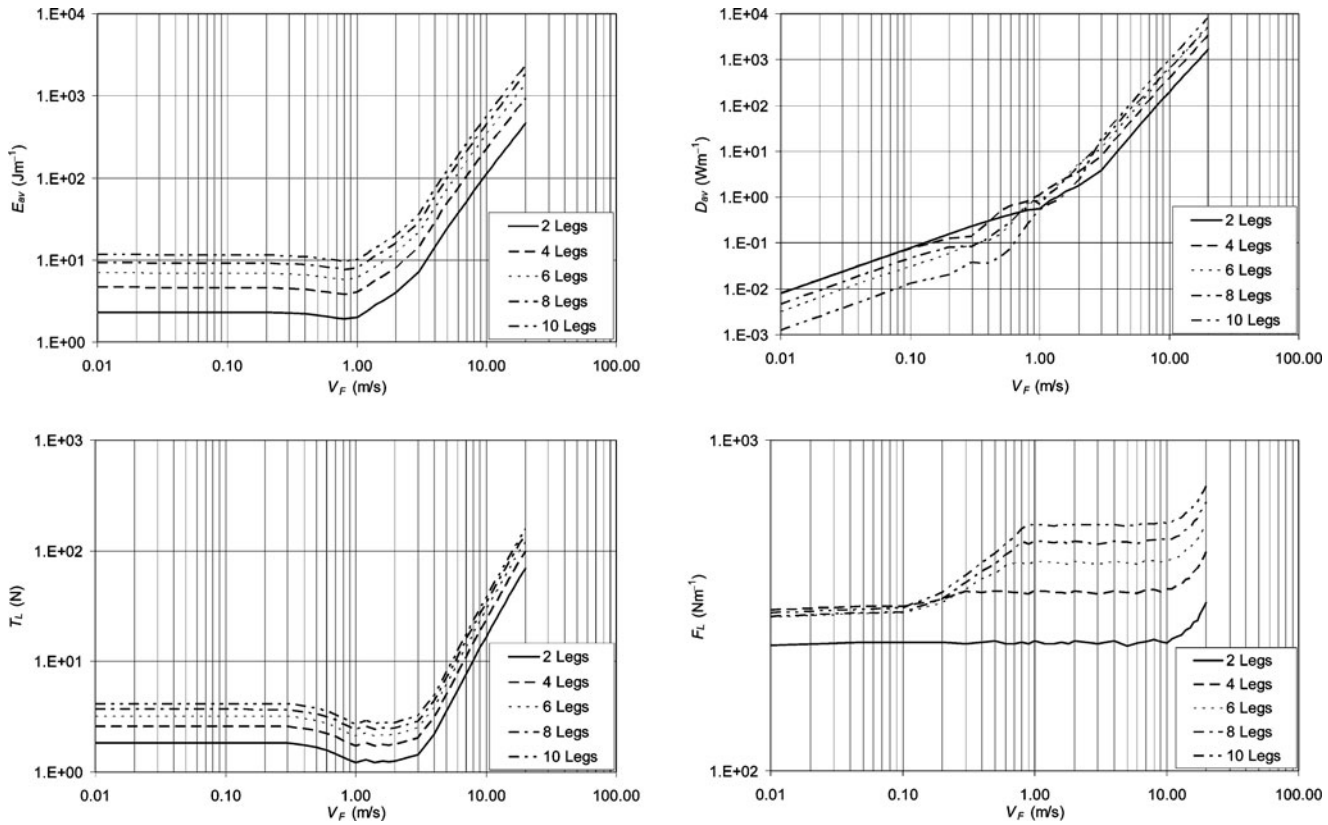


Fig. 29. Charts of min$[E_{av}(V_F)]$, min$[D_{av}(V_F)]$, min$[T_L(V_F)]$ and min$[F_L(V_F)]$, for several number of robot legs $n = \{2, 4, 6, 8, 10\}$, with $F_C = 0.01$ m, WG.

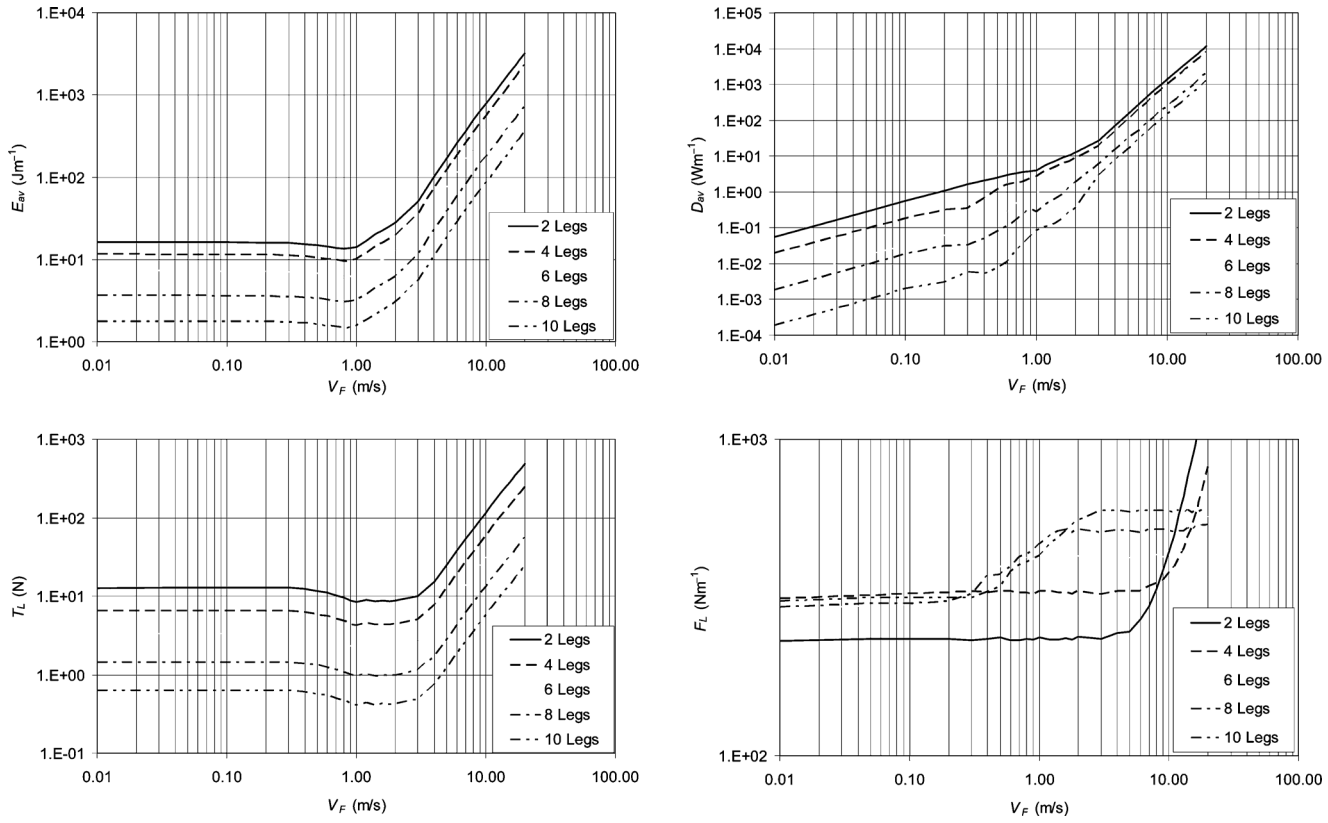


Fig. 30. Charts of min$[E_{av}(V_F)]$, min$[D_{av}(V_F)]$, min$[T_L(V_F)]$ and min$[F_L(V_F)]$, for various number of robot legs $n = \{2, 4, 6, 8, 10\}$, with $F_C = 0.01$ m, WG.

https://doi.org/10.1017/S0263574707003554 Published online by Cambridge University Press

6. Discussion of the Results

The difference between the observations in nature and the results obtained with the simulations can be explained as follows. For high velocities, animals change from walking gaits to running gaits. Running leads to higher velocities than walking, and explores the dynamics to negotiate very spaced footprints (horizontally or vertically). When running, a machine (or an animal) exhibits flight periods during which the contact with the ground is totally lost. Generally, running is a dynamic phenomenon where the inertial forces are significant and balance is achieved through active processes, and not through a static balance.

In fact, it is recognized that during running there is an increase of the energy consumption to accelerate and decelerate the centre of mass of the animal's body; this is related to the ballistic phase of the flight (Lapshin, 1995). However, it is verified that for high velocities the main part of the energy consumption is related to the maintenance of the legs oscillatory motion. Animals reduce this energy consumption by changing to dynamic locomotion modes and by running, which allows them to increase the relative duration of the leg transfer phase (decreasing the value of the duty factor β). Additionally, animals use the elastic properties of muscles and tendons for recovering energy during locomotion. The elastic effects are usually significant and can be explored for the cyclic storage of energy. This is known to occur and contributes to improve the performance of biological systems. These effects are not considered on the presented model.

Besides what has been exposed, the differences found among the performances of the living beings and the model simulations can be credited to a large number of aspects. An aspect that seems more likely to occur is that the model does not take into account all the effects of biological locomotion. Among them, the following can be mentioned:

- The joint actuators, assumed rotational in our model, are different from those revealed by the living beings that are linear and driven by a combination of muscles and tendons.
- In animals, particularly at medium and high velocities, the muscles and the tendons behave like parallel spring-dashpot systems. In this way, they have the ability to store potential energy resulting from the foot impact with the ground and to transform that energy into kinetic energy, which is returned immediately before the foot abandons the ground to start a new transfer phase (Alexander, 1990).
- In living beings, the centre of mass is not in the geometrical centre of the animal body but, instead, is frequently shifted to the front of the geometrical centre (Kram *et al*., 1997).
- In living beings, particularly in those with more than four legs, the functions of the legs are clearly differentiated. The middle legs are for supporting the body weight, the front ones to guide the animal and the rear ones to thrust the body (Kram *et al*., 1997). Some exploratory simulations, assuming that all legs could present different links lengths and foot trajectory offsets, point out that the hexapod rear legs remain stretched with the feet shifted back in relation to the hip, contrarily to the middle and front legs, somehow in resemblance of what occurs in some insects.

7. Conclusions and Perspectives for Future Developments

In this paper, several kinematic and dynamic aspects of multi-legged artificial locomotion systems exhibiting periodic gaits were compared. By simulating different motion patterns, it was estimated how the robot responds to a large variety of factors such as gait, duty factor, body height, step length, maximum foot clearance, legs link lengths, foot trajectory offset, robot body velocity, number of robot legs and robot body and leg mass.

For analysing the multi-legged kinematic performance, two quantitative measures were formulated, i.e. a perturbation analysis and the locomobility index. The perturbation analysis tends to be an elegant, though computationally demanding method. Its random characteristics seem to be particularly tailored for examining the role of the different variables on the locomotion process. On the other hand, the locomobility measure captures the geometric amplification between the legs joints and the feet or body trajectories.

Regarding the dynamic performance measures, four quantitative measures were formulated, i.e. the mean absolute density of energy during locomotion, the mean power density dispersion, the density of power lost in the joint actuators and the mean force at the body–legs interface, all these indices being evaluated along the locomotion cycle.

Based on the simulation results, several conclusions were obtained on the best set of robot and locomotion parameters for different walking conditions. It was concluded that the results from the kinematic criteria are in accordance with those obtained through the dynamic indices. Moreover, the results of several simulations agree with experimental results obtained from the study of biological locomotion.

Although our attention has been focused on the locomotion in the sagittal plane using periodic locomotion gaits, certain aspects of locomotion are not necessarily captured by the proposed measures.

As perspectives for future work, the following ideas are outlined that, in the authors opinion, deserve further research:

- Evaluation of the robots performance if the hip trajectories are not horizontal and executed at a constant velocity, as considered in this work. Therefore, the hips may exhibit some oscillation as it is verified in biological systems; as observed by Alexander (1984), most legged locomotion animals optimise the energy efficiency in opposition to motion smoothness
- Performance analysis of artificial locomotion systems in case the hexapod leg pairs (front, middle and rear) have different dimensions and distinct hip trajectory offsets, as occuring in animals, particularly in insects (Kram *et al*., 1997)
- Study of the robots performance in case the joint trajectories are determined by central pattern generators
- Performance evaluation if the leg actuation has mechanisms that allow the storage of energy during the foot impact with the ground for recovery during the transfer phase

https://doi.org/10.1017/S0263574707003554 Published online by Cambridge University Press

- System analysis if the actuators are linear, with two elements per joint, with agonist-antagonist effects as verified with the muscles actuating the joints of biological systems (Vanderborght *et al*., 2006);
- Experimentation of linear actuators such as pneumatic muscle-like actuators (based on McKibben muscles), shape memory alloys actuators or artificial polymers.

References

Alexander, R. McN, "The gaits of bipedal and quadrupedal animals," *Int. J. Robot. Res.* **3**(2), 49–59 (1984).

Alexander, R. McN, "Three uses for springs in legged locomotion," *Int. J. Robot. Res.* **9**(2), 53–61 (1990).

Briskin, E. S., Chernyshev, V. V. and Maloletov, A. V., "On Conception of Walking Machines Designing," *Proceedings of the 11th International Conference on Advanced Robotics* (2003) pp. 1763–1768.

Campbell, D. and Buehler, M. "Stair Descent in the Simple Hexapod 'RHex'," *Proceedings of the 2003 IEEE International Conference on Robotics and Automation* (2003) pp. 1380–1385.

Cham, J. G., Bailey, S. A., Clark, J. E., Full, R. J. and Cutkosky, M. R., "Fast and robust: Hexapedal robots via shape deposition manufacturing," *Int. J. Robot. Res.* **21**(10–11), 869–882 (2002).

Farritor, S., Dubowsky, S., Rutman, N. and Cole, J., "A systems-level modular design approach to field robotics," *Proceedings of the 1996 IEEE International Conference on Robotics and Automation* (1996) pp. 2890–2895.

Fedak, M. A., Heglund, N. C. and Taylor, C. R., "Energetics and mechanics of terrestrial locomotion: II. Kinetic energy changes of the limbs and body as a function of speed and body size in birds and mammals," *J. Exp. Biol.***79,** 23–40 (1982).

Gabrielli, G. and Von Kármán, T., "What price speed? Specific power required for propulsion of vehicles," *Mech. Eng.*, 775–781 (1950).

Garcia, E. and de Santos, P. G., "An improved energy stability margin for walking machines subject to dynamic effects," *Robotica* **23**(1), 13–20 (2005).

Habumuremyi, J.-C. and Doroftei, I., "Mechanical Design and MANFIS Control of a Leg for a New Demining Walking Robot," *Proceedings of the 4th International Conference on Climbing and Walking Robots* (2001) pp. 457–464.

Heglund, N. C., Cavagna, G. A. and Taylor, C. R., "Energetics and mechanics of terrestrial locomotion: III. Energy changes of the centre of mass as a function of speed and body size in birds and mammals," *J. Exp. Biol.* **79**, 41–56 (1982).

Hirose, S., Yoneda, K. and Tsukagoshi, H., "TITAN VII: Quadruped Walking and Manipulating Robot on a Steep Slope," *Proceedings of the 1997 IEEE International Conference on Robotics and Automation* (1997) pp. 494–500.

Hirose, S. and Arikawa, K., "Coupled and Decoupled Actuation of Robotic Mechanisms," *Proceedings of the 2000 IEEE International Conference on Robotics and Automation* (2000) pp. 33–39.

Ishiguro, A., Kawasumi, K. and Fujii, A., "Increasing Evolvability of a Locomotion Controller Using a Passive-Dynamic-Walking Embodiment," *Proceedings of the 2002 IEEE/RSJ International Conference on Intelligent Robots and Systems* (2002) pp. 2581–2586.

Juárez-Guerrero, J., Muñoz-Gutiérrez, S. and Mayol Cuevas, W. W., "Design of a Walking Machine Structure Using Evolutionary Strategies," *Proceedings of the 1998 IEEE International Conference on Systems, Man and Cybernetics* (1998) pp. 1427–1432.

Kajita, S., Nagasaki, T., Yokoi, K., Kaneko, K. and Tanie, K., "Running Pattern Generation for a Humanoid Robot," *Proceedings of the 2002 IEEE International Conference on Robotics and Automation* (2002) pp. 2755–2761.

Kang, T., Kim, H., Son, T. and Choi, H., "Design of Quadruped Walking and Climbing Robot," *Proceedings of the 2003 IEEE/RSJ International Conference on Intelligent Robots and Systems* (2003) pp. 619–624.

Koyachi, N., Arai, T., Adachi, H., Murakami, A. and Kawai, K., "Mechanical Design of Hexapods With Integrated Limb Mechanism: MELMANTIS-1 and MELMANTIS-2," *Proceedings of 8th International Conference on Advanced Robotics* (1997) pp. 273–278.

Kram, R., Wong, B. and Full, R. J., "Three-dimensional kinematics and limb kinetic energy of running cockroaches,"*J. Exp. Biol.* **200**, 1919–1929 (1997).

Laksanacharoen, S., Pollack, A. J., Nelson, G. M., Quinn, R. D. and Ritzmann, R. E., "Biomechanics and Simulation of Cricket for Microrobot Design," *Proceedings of the 2000 IEEE International Conference on Robotics and Automation* (2000) pp. 1088–1094.

Lapshin, V. V., "Energy Consumption of a Walking Machine. Model Estimations and Optimization," *Proceedings of the 7th International Conference on Advanced Robotics* (1995) pp. 420–425.

Lasa, M. de and Buehler, M., "Dynamic Compliant Quadruped Walking," *Proceedings of the 2001 IEEE International Conference on Robotics and Automation* (2001) pp. 3153–3158.

Leger, C., *DARWIN2K—An Evolutionary Approach to Automated Design for Robotics* (Kluwer, New York, 2000).

Linde, R. Q. van der, "Active Leg Compliance for Passive Walking," *Proceedings of the 1998 IEEE International Conference on Robotics and Automation* (1998) pp. 2339–2344.

Marhefka, D. W. and Orin, D. E., "Gait Planning for Energy Efficiency in Walking Machines," *Proceedings of the 1997 IEEE International Conference on Robotics and Automation* (1997) pp. 474–480.

Moore, E. Z., Campbell, D., Grimminger, F. and Buehler, M., "Reliable Stair Climbing in the Simple Hexapod 'RHex'," *Proceedings of the 2002 IEEE International Conference on Robotics and Automation* (2002) pp. 2222–2227.

Neuhaus, P. and Kazerooni, H., "Design and Control of Human Assisted Walking Robot," *Proceedings of the 2000 IEEE International Conference on Robotics and Automation* (2000) pp. 563–569.

Pedroche, T. A. G., Ruiz, M. A. J. and Santos, P. G. de, "A Detailed Power Consumption Model for Walking Robots," *Proceedings of the 6th International Conference on Climbing and Walking Robots* (2003) pp. 235–242.

Saranli, U., Buehler, M. and Koditschek, D. E., "RHex—A simple and highly mobile hexapod robot," *Int. J. Robot. Res.* **20**(7), 616–631 (2001).

Silva, M. F., Machado, J. A. T. and Lopes, A. M., "Modelling and simulation of artificial locomotion systems," *Robotica* **23**(5), 595–606 (2005).

Silva, M. F. and Machado, J. A. T., "An historical perspective of legged robots," *J. Vibr. Control* (2007) to be published.

Silva, M. F., Machado, J. A. T. and Lopes, A. M., "Performance Analysis of Multi-Legged Systems," *Proceedings of the 2002 IEEE International Conference on Robotics and Automation* (2002) pp. 2234–2239.

Silva, M. F., Machado, J. A. T. and Lopes, A. M., "Power Analysis of Multi-Legged Systems," *Proceedings of the 15th IFAC World Congress on Automatic Control* (2002).

Silva, M. F., Machado, J. A. T. and Lopes, A. M., "Gait Analysis of Natural and Artificial Walking Systems," **In:** *Intelligent Systems at the Service of Mankind–Volume I* (W. Elmenreich, J. T. Machado and I. J. Rudas eds.) (Ubooks, Augsberg, Germany, 2003) pp. 87–98.

Takeuchi, H., "Development of "MEL HORSE"," *Proceedings of the 1999 IEEE International Conference on Robotics and Automation* (1999) pp. 1057–1062.

Taylor, C. R., Heglund, N. C. and Maloiy, G. M. O., "Energetics and mechanics of terrestrial locomotion: I. Metabolic energy consumption as a function of speed and body size in birds and mammals," *J. Exp. Biol.* **79**, 1–21.

https://doi.org/10.1017/S0263574707003554 Published online by Cambridge University Press

Vanderborght, B., Verrelst, B., Van Ham, R. and Lefeber, D., "Controlling a bipedal walking robot actuated by pleated pneumatic artificial muscles," *Robotica* **24**(4), 401–410 (2006).

Witte, H., Hackert, R., Fischer, M. S., Ilg, W., Albiez, J., Dillmann, R. and Seyfarth, A., "Design Criteria for the Leg of a Walking Machine Derived by Biological Inspiration from Quadrupedal Mammals," *Proceedings of the 4th International Conference on Climbing and Walking Robots* (2001) pp. 63–68.

Witte, H., Hackert, R., Lilje, K. E., Schilling, N., Voges, D., Klauer, G., Ilg, W., Albiez, J., Seyfarth, A., Germann, D., Hiller, M., Dillmann, R. and Fischer, M. S., "Transfer of Biological Principles into the Construction of Quadruped Walking Machines," *Proceedings of the Second International Workshop on Robot Motion and Control* (2001) pp. 245–249.

Yang, J. M., "Fault-tolerant crab gaits and turning gaits for a hexapod robot," *Robotica* **24**(2), 269–270 (2006).

Yoshikawa, T., *Foundations of Robotics–Analysis and Control* (MIT Press, Cambridge, 1990).

Zhoga, V. V., "Computation of Walking Robots Movement Energy Expenditure," *Proceedings of the 1998 IEEE International Conference on Robotics and Automation* (1998) pp. 163–168.

Zhou, Y., "On the planar stability of rigid-link binary walking robots," *Robotica* **21**(6), 667–675 (2003).

https://doi.org/10.1017/S0263574707003554 Published online by Cambridge University Press